In: The Journal of Physiology (2017)
http://dx.doi.org/ 10.1113/JP275413
Manuscript as accepted

Hyperexcitability of the network contributes to synchronization processes in the human epileptic neocortex.

Kinga Tóth1,2*, Katharina T. Hofer1,3*, Ágnes Kandrács1,3, László Entz4, Attila Bagó4, Loránd Erőss4, Zsófia Jordán4, Gábor Nagy4, András Sólyom4, Dániel Fabó4, István Ulbert1,3,4 and Lucia Wittner1,2,4

1. Institute of Cognitive Neuroscience and Psychology, Research Center for Natural Sciences, Hungarian Academy of Sciences, 1117 Budapest, Hungary

2. Institute of Experimental Medicine, Hungarian Academy of Sciences, 1083 Budapest, Hungary

3. Department of Information Technology, Pázmány Péter Catholic University, 1083 Budapest, Hungary

4. National Institute of Clinical Neuroscience, 1143 Budapest, Hungary

* These authors contributed equally.

Correspondence to:
Lucia Wittner
Institute of Cognitive Neuroscience and Psychology,
Research Center for Natural Sciences, Hungarian Academy of Sciences,
1117 Budapest, Magyar tudósok körútja 2. Hungary
tel: +36-1-382-6807
e-mail: wittner.lucia@ttk.mta.hu
ORCID ID: 0000-0001-6800-0953

Running head: Spontaneous network events in human neocortex

Abstract

Interictal activity is a hallmark in epilepsy diagnostics and is linked to neuronal hypersynchrony. Little is known about perturbations in human epileptic neocortical microcircuits, and their role in generating pathological synchronies. To explore hyperexcitability of the human epileptic network, and its contribution to convulsive activity, we investigated an in vitro model of synchronous burst activity spontaneously occurring in postoperative tissue slices derived from patients with or without preoperative clinical and electrographic manifestations of epileptic activity. Human neocortical slices generated two types of synchronies. Interictal-like discharges (classified as epileptiform events) emerged only in epileptic samples, and were hypersynchronous bursts characterized by considerably elevated levels of excitation. Synchronous population activity was initiated both in epileptic and non-epileptic tissue, with a significantly lower degree of excitability and synchrony, and could not be linked to epilepsy. However, in pharmacoresistant epileptic tissue, higher percentage of slices exhibited population activity, with higher local field potential gradient amplitudes. More intracellularly recorded neurons received depolarizing synaptic potentials, discharging more reliably during the events. Light and electron microscopic examinations showed slightly lower neuron densities, and higher densities of excitatory synapses in the human epileptic neocortex. Our data suggest that human neocortical microcircuits retain their functionality and plasticity in vitro, and can generate two significantly different synchronies. We propose that population bursts might not be pathological events while interictal-like discharges may reflect the epileptogenicity of the human cortex. Our results show that hyperexcitability characterizes the human epileptic neocortical network, and that it is closely related to the emergence of synchronies.

Key points summary

- Hyperexcitability and hypersynchrony of neuronal networks are thought to be linked to the generation of epileptic activity both in humans and animal models.
- Here we show that human epileptic postoperative neocortical tissue is able to generate two different types of synchronies, in vitro.
- Epileptiform bursts occurred only in slices derived from epileptic patients and were hypersynchronous events characterized by high levels of excitability.
- Spontaneous population activity emerged both in epileptic and non-epileptic tissue, with a significantly lower degree of excitability and synchrony, and could not be linked to epilepsy.
- These results help us better understand the role of excitatory and inhibitory neuronal circuits in the generation of population events, and to define the subtle border between physiological and pathological synchronies.

Keywords

epilepsy, oscillation, neuronal circuits, neocortex, interictal discharges

Abbreviations

CSD: current source density

EEG: electroencephalogram

HFO: high frequency oscillation

IID: interictal-like discharge

LFPg: local field potential gradient

MUA: multiple unit activity

SPA: spontaneous synchronous population activity

Introduction

Epilepsies are characterized by the presence of interictal spikes detected on scalp electroencephalographic (EEG) recordings, which are considered to reflect hypersynchronous and wide spread activation of neuronal circuits. Interictal discharges in both human and experimental focal epilepsies were described as high amplitude, fast EEG spikes followed by a slow wave (de Curtis & Avanzini, 2001). In vivo human experiments showed that neocortical interictal spikes were either generated locally, or propagated from distant sites, both with an initial current sink and a considerable increase in cellular firing (Ulbert *et al.*, 2004a).

Substantial effort has been made to reveal whether the resected human cortical tissue retains its ability to generate convulsive activity if maintained in vitro (for review see Avoli *et al.*, 2005). Spontaneous synchronous discharges are known to be generated by slices prepared from the human epileptic neocortex (McCormick, 1989; Köhling *et al.*, 1998; Gorji *et al.*, 2002; Roopun *et al.*, 2010; Pallud *et al.*, 2014) or the hippocampal formation (Cohen *et al.*, 2002; Wozny *et al.*, 2005; Huberfeld *et al.*, 2007; Wittner *et al.*, 2009; Huberfeld *et al.*, 2011) in a physiological perfusion solution. When filtered as the EEG (1-100 Hz), the waveform of in vitro events (Cohen *et al.*, 2002) resembled in vivo interictal discharges (Ulbert *et al.*, 2004a; Fabó *et al.*, 2008). Other similarities include the increase of cellular activity and fast oscillations seen in wide band (1-3000 Hz) filtering (Wittner *et al.*, 2009; Simon *et al.*, 2014). Intracellularly, synchronous population events were reflected as large, complex postsynaptic potentials with or without synchronous cell firing (Schwartzkroin & Knowles, 1984; McCormick, 1989; Wittner *et al.*, 2009; Pallud *et al.*, 2014), involving both excitatory and inhibitory signaling (Schwartzkroin & Haglund, 1986; Köhling *et al.*, 1998; Cohen *et al.*, 2002). These postsynaptic potentials were found more frequently in neurons deriving from the

epileptogenic zone than in those from adjacent neocortical tissue (Schwartzkroin & Knowles, 1984). Since synchronous bursts could not be detected in non-primate neocortical slices (Köhling *et al.*, 1998), and healthy human control is lacking for ethical reasons, most groups believed that they might be epilepsy related phenomena (Cohen *et al.*, 2002; Huberfeld *et al.*, 2007; Roopun *et al.*, 2010; Huberfeld *et al.*, 2011; Pallud *et al.*, 2014). However, similar synchronous events were generated by healthy monkey hippocampal tissue, as detected in intracellular records (Schwartzkroin & Haglund, 1986), and could also be evoked in human non-epileptic neocortical tissue by activating single pyramidal cells (Molnár *et al.*, 2008; Szegedi *et al.*, 2016), suggesting that synchronous population activity is not necessarily related to epileptic processes.

The impaired balance of excitation and inhibition is the most conventional theory underlying interictal spike generation. Most of our knowledge about the cellular and network basis of cortical hyperexcitability comes from animal models (for review see McCormick & Contreras, 2001). Human focal cortical epilepsy is extensively studied in the limbic structures, and a wide range of data is available concerning the cellular properties of neocortical neurons (for review see Avoli *et al.*, 2005). Prolonged depolarizations, all-or-none and graded bursts could be evoked by electrical stimulation in a subset of human neocortical neurons located in the epileptogenic area verified either by electrocorticography (Prince & Wong, 1981; Avoli & Olivier, 1989), or by imaging techniques (Strowbridge *et al.*, 1992; Williamson *et al.*, 2003). Signs of network hyperexcitability were found in the 4-aminopyridine model of ictal activity generated by human slices from patients with focal cortical dysplasia (for review see Avoli *et al.*, 2005). Anatomical findings also support the presence of excess excitation in the epileptic neocortex. Higher numbers of excitatory axon terminals and a loss of inhibitory synapses were found in the neocortex of patients with temporal lobe epilepsy (Marco & DeFelipe, 1997), as well as perturbed densities of excitatory-inhibitory synapses in areas of focal

cortical dysplasia (Alonso-Nanclares *et al.*, 2005). Although the cellular properties underlying hyperexcitability have been widely explored in the human neocortex, little is known about how an impaired balance of excitation and inhibition of the neuronal network contributes to epileptic hypersynchrony in humans.

The question of control tissue is always problematic in case of human studies. Anatomical studies usually include human autopsy tissue as control (for example: Tóth *et al.*, 2010), while electrophysiological studies typically operate with healthy monkey (Schwartzkroin & Haglund, 1986) or rodent tissue (Köhling *et al.*, 1998; Heinemann *et al.*, 2000), sometimes together with its corresponding epilepsy model (for example Lehmann *et al.*, 2000). Furthermore, sclerotic hippocampus is usually compared to non-sclerotic hippocampus derived from epileptic patients (Isokawa & Fried, 1996; Kivi *et al.*, 2000; Gabriel *et al.*, 2004; Williamson *et al.*, 2005), and epileptogenic neocortex surrounding epileptogenic lesions is compared to adjacent, non-affected areas (Strowbridge *et al.*, 1992; Williamson *et al.*, 2003; Alonso-Nanclares *et al.*, 2005; Thom *et al.*, 2005). The best control available for human epileptic neocortex, i.e. tissue from non-epileptic patients, has been investigated in only one intracellular study so far (Prince & Wong, 1981).

In the present work, we used spontaneous population bursts emerging in human neocortical slices as a network model for synchrony to examine excitatory processes contributing to epileptic activity. We demonstrate that excess excitation is present at the network level in the human epileptic neocortex compared to tissue derived from tumour patients without any preoperative clinical or electrographic appearances of seizures. We show that human neocortical slices can generate two distinct types of synchronous activities. Based on their occurrence and network characteristics we conclude that synchronous population activity (SPA) does not seem to be related to epileptic processes, whereas interictal-like

discharges (IID) seem to be associated to epilepsy. The anatomical and physiological differences of neocortical networks between humans and animals are also discussed.

Materials and methods

Patients

All patients gave written consent, and our protocol was approved by the Hungarian Ministry of Health. The study was approved by the Regional and Institutional Committee of Science and Research Ethics of Scientific Council of Health (ETT TUKEB 20680-4/2012/EKU) and performed in accordance with the Declaration of Helsinki.

Epileptic patients

Epileptic tissue samples were obtained from 49 patients (Table 1). We obtained epileptic neocortical tissue from frontal (n=15 patients), temporal (n=25 patients), parietal (n=5 patients) and occipital (n=4 patients) lobes. Most of the patients (n=26) suffered from focal cortical epilepsy for 19.6±14.6 years on average. The scalp EEG showed the presence of interictal spikes in all these patients. The remaining 23 patients had brain tumours, and had recurrent epileptic seizures (n=12 patients) for 6.0±6.0 years on average, or had only one seizure (or status epilepticus) within 10±22 months prior their surgery (n=11 patients) and were therefore considered to be epileptic. Seventeen patients suffering from epilepsy+tumour had tumours of glial origin. Three of these 17 patients were operated for their glial tumour earlier, and now underwent their second operation to resect necrotic brain tissue caused by radiotherapy. Four patients had carcinoma metastasis. Two patients had other types of tumour (see Table 1). Thirteen epileptic patients were diagnosed with cortical dysgenesis, they were epileptic for 20.2±12.7 years on average. Focal cortical dysplasia was found in nine patients, two of them also suffered from hippocampal sclerosis. Four patients showed signs of other cortical dysgenesis. Hippocampal sclerosis was detected in 8 patients, who were epileptic for 25.8±16.7 years on average. The remaining five patients had cavernoma (n=4) or viral

encephalitis (n=1), and were classified as “other”. The duration of epilepsy of these five patients was 8.0±10.3 years. Epileptic patients: 24 females, 25 males, age range: 18-72 years, mean±st.dev.: 40.1±16.1 years.

Non-epileptic patients

Thirty-three patients diagnosed with brain tumour but without epilepsy were included in this study (Table 1). These patients – as it is stated in their anamnesis – did not survive clinical manifestation of epileptic seizure before the date of their brain surgery. Preoperative clinical EEG recordings confirmed in eight of these patients that no electrographic signs of epileptic activity were present on their scalp EEG. We obtained non-epileptic neocortical specimens from frontal (n=10 patients), temporal (n=11 patients), parietal (n=7 patients) and occipital (n=5 patients) lobes. Fourteen patients were diagnosed with tumours of glial origin: glioblastoma (n=12) or anaplastic astrocytoma (n=2). Fourteen patients had carcinoma metastasis. The remaining five patients were operated for other reasons (for details see Table 1). The distance of the obtained neocortical tissue from the tumour has been provided by the neurosurgeon, based on magnetic resonance (MR) images, intraoperative pictures and occasionally defined by navigational system. Non-epileptic patients: 18 females, 15 males, age range: 31-82 years, mean±st.dev.: 61.7±11.7 years.

Tissue preparation

Tissue was transported from the operating room to the laboratory (located in the same building) in a cold, oxygenated solution containing (in mM) 248 D-sucrose, 26 $NaHCO_3$, 1 KCl, 1 $CaCl_2$, 10 $MgCl_2$, 10 D-glucose and 1 phenol red, equilibrated with 5% CO_2 in 95% O_2. Neocortical slices of 500 µm thickness were cut with a vibratome. They were transferred and maintained at 35–37°C in an interface chamber perfused with a standard solution

containing (in mM) 124 NaCl, 26 $NaHCO_3$, 3.5 KCl, 1 $MgCl_2$, 1 $CaCl_2$, and 10 D-glucose, equilibrated with 5% CO_2 in 95% O_2.

Recordings

Intracellular recordings were made with microelectrodes that contained 2M KAc with a resistance of 50–100 MΩ. The data were obtained within 10–20 min of penetration. Signals were amplified with a BA-1S amplifier (NPI Electronic GmbH, Tamm, Germany) operated in current-clamp mode. In acceptable records, the membrane potential was more negative than -50 mV, input resistance was higher than 20 MΩ, and action potentials were overshooting.

The extracellular local field potential gradient (LFPg) was recorded with a laminar multiple channel (24 channels, distance between contacts: 150 µm) microelectrode (Ulbert *et al.*, 2001; Ulbert *et al.*, 2004a; Ulbert *et al.*, 2004b; Fabó *et al.*, 2008; Wittner *et al.*, 2009), using a custom made 48-channel voltage gradient amplifier of pass-band 0.01 Hz to 10 kHz. Signals were digitized with a 32 channel, 16-bit resolution analog-to-digital converter (National Instruments, Austin TX, USA) at 20 kHz sampling rate, recorded with a home written routine in LabView7 (National Instruments, Austin TX, USA). The linear 24 channel microelectrode was placed perpendicular to the pial surface, and slices were mapped from one end to the other at every 300-400 µm.

Drugs

A type γ-aminobutyric acid ($GABA_A$) receptor mediated signaling was suppressed by bicuculline methiodide (10 µM). AMPA (α-amino-3-hydroxyl-5-methyl-4-isoxazole-propionate) and KA (kainate) type glutamate receptors were blocked using 2,3-dihydroxy-6-nitro-7-sulfamoyl-benzo(f)quinoxaline (5 µM, NBQX) and NMDA (N-methyl-D-aspartate)

type receptors were blocked with DL-2-amino-5-phosphonovaleric acid (50 µM, DL-APV). Drugs were obtained from Tocris Bioscience (Izinta Kft., Hungary).

Data analysis

Data were analyzed with the Neuroscan Edit4.5 program (Compumedics Neuroscan, Charlotte, NC, USA), and home written routines for Matlab (The MathWorks, Natick, MA, USA). Current source density (CSD), an estimate of population trans-membrane currents, and multiple unit activity (MUA) were calculated from the LFPg using standard techniques (Ulbert *et al.*, 2001; Ulbert *et al.*, 2004b; Wittner *et al.*, 2009). Baseline correction (-150 to -50 ms) was applied to averaged LFPg, CSD and MUA. In the color maps, CSD sinks are presented in red, sources in blue. Warm colors (red) depict MUA-increases and cold colors (blue) depict MUA decreases compared to baseline.

Synchronous activity (SPA and IID) detection was performed on LFPg records after a double Hamming window spatial smoothing and a band-pass filtering between 3 and 30 Hz (zero phase shift, 12 dB/octave). The peak of the LFPg transient was detected with a routine in Matlab, and was considered as time zero for further event triggered averaging. Events larger than 3x standard deviation were detected and included in the analyses. The location of SPAs/IIDs was determined in each case. The 24-channel microelectrode covered all layers of the neocortex in almost all cases. Usually channels 1-8 were in the supragranular, channels 9-13 in the granular and channels 14-23 were in the infragranular layers. Channel positions were determined according to the thickness of the neocortex of the given patient, and corrected if necessary. Waveform analysis was performed on averaged synchronous activities with a home written C++ routine.

Ripple and fast ripple components of SPAs and IIDs were determined with the aid of routines written in Matlab, as follows. Original 20 kHz sampling rate records were down

sampled to 2000 Hz. Wavelet analysis was applied on epochs containing 4096 sampling points (from -1000 ms to 1047 ms) with the LFPg peak of the SPA/IID at time zero (detected as above). Time-frequency analysis was performed between 0 and 800 Hz on the electrode channels where SPA was present, and baseline corrected to -300 to -100 ms. We systematically saw a peak around 200 Hz, and therefore we modified the conventional limit of 200 Hz for ripple frequency (Bragin *et al.*, 1999) to 250 Hz. For each channel, the maximal power change (relative to the baseline) was determined within the range of 130 to 250 Hz (ripple frequency) and 300 to 800 Hz (fast ripple frequency) at time zero (i.e. at the time point of the LFPg peak of the SPAs/IIDs). The frequencies where the power showed the maximum were also determined. Both the ripple and fast ripple power and frequencies were averaged across channels, to receive one ripple and one fast ripple power and frequency parameter for each recording. This last step was needed for the comparison of recordings with population activities spreading to different numbers of channels.

Anatomy

Intracellularly recorded cells were labelled, processed and reconstructed in three dimensions as described earlier (Wittner *et al.*, 2009).

Immunohistochemical procedures were used to verify the laminar structure and the possible tumour infiltration or signs of dysgenesis in the neocortex of 28 epileptic and 13 tumour patients. Either tissue blocks or neocortical slices following electrophysiological recording were fixed and processed as described earlier (Wittner *et al.*, 2009). Neuronal cell bodies were stained with NeuN antibody (1:2000, EMD Millipore, Billerica, MA, USA, RRID:AB_2298772), astroglial cells were stained with glial fibrillary acidic protein antibody (1:2000, EMD Millipore, Billerica, MA, USA, RRID:AB_94844), and perisomatic inhibitory cells were marked with parvalbumin antibody (1:7000, Swant, Bellinzona, Switzerland,

RRID:AB_10000343). All antibodies were mouse monoclonal antibodies. Their specificity was tested by the manufacturer. Visualization of immunopositive elements was performed as described earlier (Wittner *et al.*, 2009).

The total cell density and the synaptic connectivity were examined in regions which generated SPA and in neighboring regions that did not show SPA. The following criteria were taken into consideration when choosing the samples for quantitative analysis: the site that generated SPA and the site that did not generate SPA should be part of the same slice. The NeuN- or the PV-stained sections chosen for cell counting should contain the whole length of the slice, and the whole width of the cortex, including all layers. Two slices were chosen both from tumour (patients T17 and T23) and epileptic (patients E13 and E16) subjects for NeuN+ neuron counting. Four slices from three epileptic patients (E12, E13 and E15), and three slices from three non-epileptic patients (T17, T20 and T23) for counting PV+ cell bodies. Two regions were marked including all layers: one where SPA was detected and another where recordings did not show SPA. The areas of all neocortical layers were measured, and NeuN- or PV-positive somata were counted in both regions with the aid of the NeuroLucida system (MicroBrightField Inc. Williston, VT, USA), at a magnification of 40x.

After light microscopic examination, areas of interest were re-embedded and sectioned for electron microscopy. Ultrathin serial sections were collected on Formvar-coated single slot grids, stained with lead citrate, and examined with a Hitachi 7100 electron microscope. Electron microscopic analysis was made only on specimens with high quality ultrastructural preservation. For the analysis of synaptic connectivity three slices from epileptic (E12, E13, E15) and three from non-epileptic (T17, T20, T23) patients were selected. SPA occurred in the supragranular layers in all selected slices. Two blocks were re-embedded from the supragranular layers (upper layer III) of each slice, one from the spot where SPA was recorded and the other from an area where SPA was not generated. Photos were

systematically taken at 20 000x magnification, from one side to the other side of the block without overlapping areas, to avoid multiple sampling of the same synapse. The number of the examined spots varied between 22 and 39 among the samples, with an area of 30.57 μm^2 per spot. Neuronal and glial somata were excluded from the examined area, so, all values are given relative to the neuropil. The values of the examined area from each block varied between 2200 and 3400 μm^2. The number of asymmetrical (presumably excitatory) and symmetrical (presumably inhibitory) synapses were determined per 100 μm^2 in each region.

Statistical analysis

Our data sets were not following Gaussian distributions, therefore non-parametric tests were used. The Mann-Whitney U test was used when two groups; Kruskal-Wallis ANOVA was used when more than two groups were compared. In case of the latter, differences between groups were determined via post-hoc tests provided by Matlab. In case of multiple testing, p-values were corrected using the Bonferroni-Holm method.

For testing the effect of DL-APV we used the paired Wilcoxon signed rank test.

For contingency tables the Fisher exact test or Chi square test were used, if the expected values were low or high, respectively.

P-values below 0.05 were considered to be statistically significant.

Results

Occurrence of synchronous population activity

Synchronous population activity (SPA) was spontaneously generated in a standard bathing solution in slices from both epileptic (n=133/287 slices, 46.3% in n=43/49 patients) and non-epileptic patients (n=60/194 slices, 30.9% in n=24/33 patients, significantly different, p<0.05, Fig. 1, for patient data see Methods and Table 1). In several cases (n=9 activities, 3.1%, in n=7/287 slices, in n=5/49 epileptic patients), considerably larger and more complex bursts also emerged in the neocortex derived only from epileptic patients (Fig. 1G). They resembled epileptiform population bursts induced by 4-amino-pyridine (Avoli *et al.*, 1994), and were therefore named interictal-like discharges (IID, see Fig. 1), and analysed separately. When separating IIDs from SPAs we considered every examined network features of the synchronous activities: layer of emergence, recurrence frequency, local field potential gradient (LFPg), current source density (CSD) and multiple unit activity (MUA) amplitude (see later in details). LFPg and CSD amplitude are related to each other, since CSD is the first derivative of LFPg signal (see Methods). LFPg gives the difference in local field potential between two neighbouring electrode contacts, and might be misrepresentative in case of synchronies spreading to higher numbers of contacts. In contrast, CSD amplitude gives an estimate of transmembrane current amplitude, independent from the spatial dimensions of the synchrony. Moreover, MUA amplitude can be misleading if a large amplitude single unit with related firing to the synchrony is visible on the trace. All these technical considerations were taken into account when establishing our categories. Although each property showed slightly overlapping values, combining all parameters gave a clear distinction between SPAs and IIDs. We combined CSD and MUA, to be able to visualise the examined features in a three-dimensional plot (Fig. 1J).

SPA occurrence was similar in slices derived from different lobes (Table 2, p>0.1 and p>0.8 in epileptic and tumour tissue, respectively), but was significantly higher in tissue resected from patients with epilepsy than in slices derived from non-epileptic patients (p<0.01). SPA was generated at a significantly lower rate in slices from epileptic patients with tumour (n=23, 36.4±29.0%, mean±standard deviation) than from epileptic patients with dysgenesis (n=13), hippocampal sclerosis (n=8), or other associated symptoms (n=5, varying from 50.3±34.0% to 58.3±28.6%, p<0.05, Table 3). The specimens obtained from patients with dysgenesis were classified as affected (n=46 slices from seven patients) or non-affected (n=26 slices from five patients) by the dysgenesis, based on our subsequent anatomical analysis. We found similar values of SPA emergence in the dysgenetic (n=26/46 slices, 56.5%) and in the non-dysgenetic (n=14/26 slices, 53.9%) neocortex (Chi-Square Test; p>0.8).

SPA generation was variable in patients with brain tumour, relative to their type of tumour (Table 3). The SPA occurrence rate in all tumour patients with or without preoperative epileptic seizures was 32.4±27.4%. Higher, although not significant (p>0.1) ratios were found in the cases with glial tumour (38.7±28.6%, n=31 patients), and other associated symptoms (35.0±29.0%, n=7 patients), than in brains with carcinoma metastasis (20.6±21.3%, n=12 patients). We verified how the distance of the specimen from the tumour affected SPA generation in our samples. In the cases where the resected neocortical tissue was close (<30 mm) to the tumour, 25.0±22.8% of the slices generated SPA (in n=23 patients, for determination of the distance between the tumour and the resected neocortical tissue see Methods). When the examined tissue was at higher distances from the tumour (>30 mm, but in most cases >50 mm), SPA emerged in higher percentages of the slices (36.1±27.9%, in n=31 patients), although the difference was not statistically significant (p>0.1).

Next, we wished to examine whether the different stages of epilepsy affect the ability of the neocortex to generate SPAs. Therefore, we grouped our patients (Table 1) as follows: A) patients with pharmacoresistant epilepsy; B) patients with focal or grand mal seizures who are seizure free with medication (treatable epilepsy); C) patients with one grand mal seizure or with occasional (provoked) seizures, and with no need for medication (these patients were operated for their tumour); D) patients without preoperative seizures (no epilepsy). SPA occurrence was the highest in the group with pharmacoresistant epilepsy (group A, n=33 patients): 57.0±28.0%; it was lower in the group with treatable epilepsy (group B, n=11 patients): 32.3±13.9%. We found the lowest ratios in the group with no need for medication (group C, n=5 patients): 11.7±16.2%, and in the group without epilepsy (group D, n=33 patients): 29.1±26.4%. SPA occurrence was related to the stage of epilepsy, i.e. the ratio of slices generating SPA in group A was significantly higher than in group D ($p<0.001$) or in group C ($p<0.01$).

Our above analyses show that both the presence of tumour and the stage of the patient's epilepsy influence the generation of synchronies. In this study, we wished to identify epilepsy related phenomena, which are not affected by tumour formation or by differences in the stages of epilepsy. Thus, for the analysis of network and cellular properties of the synchronies, we made three groups as follows. 1) Patients with pharmacoresistant epilepsy and without tumour (will be referred as "epileptic"). Note that this category largely overlaps with group A, but excludes patients with tumour and pharmacoresistant epilepsy. 2) Tumour patients without epilepsy (will be referred as "tumour"), this category includes patients falling into group D. 3) The remaining patients suffering from both epilepsy and tumour were pooled into the heterogeneous "epileptic+tumour" group (see Table 1). We analyzed data deriving from these groups separately, and made comparisons only between "epileptic" and "tumour" patients to draw conclusions about changes related to epilepsy.

Characteristics of SPAs and IIDs

Several types of SPAs were separated by their location and extension within the neocortex (Fig. 2A, Table 4). SPA occurred most frequently in the supragranular layers: 69.9% in epileptic, 65.2% in epileptic+tumour and 67.3% in tumour tissue (Fig. 2B, see also (Köhling *et al.*, 1998). Less often SPA could be detected in the granular and infragranular layers, and in a few cases SPA invaded the entire width of the neocortex. Interictal-like discharges (IID) emerged mainly in the deeper layers of the neocortex: granular (n=1) or in the granular+infragranular (n=5) and infragranular (n=2) layers (Fig. 2A, B, Table 4) in slices from epileptic patients, and in the supragranular+granular layers (n=1) in one slice from a patient having epilepsy+tumour.

As in a previous study (Köhling *et al.*, 1998), we observed multiple independent SPAs in the same slice. We differentiated between simultaneous multiple SPAs (Fig. 2B) or simultaneous SPA+IID (n=2 cases, Fig. 1G) at one recording site, and multiple spots of SPAs (Fig. 2C). The ratio of slices exhibiting multiple SPAs was somewhat higher in epileptic (33.3%) and epileptic+tumour (32.7%) than in tumour patients (25.0%, Table 4).

Next, the network characteristics of SPAs and IIDs emerging in the human neocortex were analyzed (Fig. 1I, Table 5). We compared SPAs emerged in epileptic slices to SPAs generated in tumour slices, as well as to IIDs detected in epileptic tissue. The recurrence frequency of SPAs was 1.20±0.71 Hz in epileptic (n=46 SPAs) and 1.18±0.63 Hz in tumour (n=48 SPAs) tissue, respectively, while that of IIDs was significantly lower (0.10±0.13 Hz, n=8 IIDs, p<0.0001). The largest amplitude on the local field potential gradient (LFPg) was significantly higher for IIDs (74.70±21.99 μV) than for SPAs (23.22±17.23 μV, p<0.0001) in the neocortex of epileptic patients, and it was significantly lower for SPAs in tumour patients (18.40±10.48 μV, p<0.01, Table 5), than for SPAs in epileptic patients. Multiple unit activity

(MUA), as an estimate of cellular firing, did not differ during SPAs in epileptic and tumour tissue (1.49±1.46 vs. 1.29±1.17 μV, respectively), but was significantly higher during IIDs (6.46±4.57 μV, $p<0.01$, Fig. 1H-I). Similar to a previous study (Köhling *et al.*, 1999), we found that the current source density (CSD) associated with the SPAs was very variable. However, in most of the cases a source-sink-source pattern was detected in the layer where the SPA occurred (Fig. 1B, D, F). The CSD pattern was usually more complex, comprising several peaks, and significantly higher in amplitude during IIDs (Fig. 1H, $p<0.0001$).

A relationship between the recurrence frequency and the field potential amplitude has been previously observed in case of population events in vitro (Papatheodoropoulos & Kostopoulos, 2002; Hofer *et al.*, 2015), i.e. as the frequency of events increases as a consequence of higher levels of $[K^+]_o$, the field potential amplitude decreases. On the other hand, this relationship could not be demonstrated in case of population bursts without changing the composition of the physiological bath solution (Hájos *et al.*, 2013). To verify this possible correlation during human neocortical synchronies, we plotted the average LFPg amplitude of SPAs/IIDs against the mean recurrence frequency or the mean inter event interval. We could not find a considerable correlation between LFPg amplitude and frequency ($R^2=0.0042$ for SPA and $R^2=0.006$ for IIDs), or inter event interval ($R^2=0.0011$ for SPAs and $R^2=0.0957$ for IIDs). However, when plotting MUA amplitude against LFPg amplitude, we found a weak correlation for SPAs ($R^2=0.3679$), indicating that larger LFPg (reflecting synaptic input, (Gulyás *et al.*, 2010) is linked to larger MUA (reflecting output). No correlation could be demonstrated in case of IIDs ($R^2=0.0135$). We also examined the relationship between the LFPg amplitude of every SPA/IID event and the length of its preceding inter event interval within each recording. In the majority of the cases (n=65/102) no significant correlation was demonstrated. In about third of the cases (n=30/102) a significant positive correlation was shown (with very weak to moderate Spearman correlation

coefficients), but we also found negative correlations (n=7/102, with very weak to weak Spearman correlation coefficients). None of the IID activities were significant, possibly due to the low IID event numbers. Altogether, correlations could be either positive or negative in both epileptic and tumour tissue, but only positive correlations showed moderate strength (data not shown).

High frequency oscillations (HFOs) were examined in the range of ripples (130-250 Hz) and fast ripples (300-800 Hz) during SPAs in slices derived from both epileptic (n=37 slices from 12 patients) and tumour patients (n=33 slices from 9 patients, Fig. 3, Table 6), as well as during IIDs in 8 recordings from epileptic patients without tumour. Simultaneous multiple SPA was present in 8/37 and 11/33 recordings, therefore 46 and 48 SPAs were examined in epileptic and tumour tissue, respectively. HFOs (mainly at ripple frequency) associated to SPAs were detected slightly (but not significantly) more frequently in slices from epileptic than from tumour patients (Table 6). Ripple frequency was significantly lower during SPAs in epileptic than in tumour tissue ($p<0.01$). Fast ripple frequency was similar in epileptic and tumour tissue, and showed slightly lower values during IIDs. Ripple and fast ripple powers during SPAs did not differ in epileptic vs. tumour tissue, but were significantly higher during IIDs ($p<0.001$ for both ripple and fast ripple powers, Table 6, Fig. 3).

Role of glutamate and GABA receptors in the generation of SPAs

To reveal the role of glutamate and GABA signaling in the generation of SPAs, we applied the AMPA/kainate glutamate receptor agonist NBQX (5 µM), or the $GABA_A$ receptor agonist bicuculline (10 µM) on human neocortical slices. As described previously (Köhling *et al.*, 1998), SPAs were reversibly suppressed by blocking either AMPA/kainate receptors (n=4 and n=5 SPAs in slices from 3 tumour and 4 epileptic patients, respectively, Fig. 2E) or $GABA_A$ receptors (n=8 and n=9 SPAs in slices from 6 tumour and 8 epileptic patients,

respectively). The role of NMDA receptors was investigated with the application of its antagonist DL-APV (50 μM), which significantly reduced the recurrence frequency of SPAs (n=4 from 3 tumour patients, n=5 from 4 epileptic patients) to 80.16 [58.63 - 99.17] % (p<0.05), and diminished the LFPg and MUA amplitudes to 90.68 [81.81 - 105.05] and 86.78 [69.53 - 110.81] %, respectively (both 0.05<p<0.1, Fig. 2E).

Intracellular correlates of SPAs

Putative pyramidal cells were intracellularly recorded in neocortical slices from epileptic (n=17) and from tumour (n=16) patients (Fig. 4, Table 7), simultaneously with the extracellular linear recordings.

Subsequent anatomical studies in case of nine cells (six from epileptic and three from tumour tissue; see Table 7) confirmed that intracellularly recorded neurons were indeed pyramidal cells. All intracellularly filled cells showed the characteristics of pyramidal cells: a triangular cell body, a long and thick apical dendrite and numerous thin basal dendrites, covered by mainly thin and mushroom spines. Four well filled cells (one from tumour tissue, three from epileptic tissue, one located in layer II, three in layer V) were reconstructed in three dimensions (Fig. 4G, H), and had an average total dendritic tree length of 34.04±9.28 mm. We should note that the real dendritic length of our human neocortical pyramidal cells was even higher, since the apical dendrite of three cells was truncated because of the slice preparation procedure.

Both the resting membrane potential and the ratio of spontaneously firing/silent cells at resting membrane potential were similar in epileptic and tumour tissue (Table 7; Mann-Whitney U Test; p=0.69 and Fisher's exact test; p=0.31, respectively).

As in previous studies (Köhling *et al.*, 1998; Roopun *et al.*, 2010; Pallud *et al.*, 2014), different types of cellular behaviors were detected during SPA (Fig. 4A-E). Cells in the

epileptic slice preparations showed either depolarizing (n=11/12 cells, 91.7%) or hyperpolarizing (n=1/12 cells, 8.3%) responses to SPA. At resting potential, seven depolarizing cells (58.3% of responding cells) also fired during SPA, at 43.5 [29.8-86.7] % of the events (median [±95% confidence interval]; Fig. 4F).

In the tumour tissue, we found neurons showing depolarizing (n=6/13 cells, 46.2%, significantly different from epileptic samples, $p<0.05$), hyperpolarizing (n=4/13 cells, 30.7%) or biphasic responses (n=3/13 cells, 23.1%), which consisted of a hyperpolarization followed by a depolarization. At resting potential, seven cells (53.8% of responding cells) also discharged during SPA. Four of these cells showed depolarizing, three showed biphasic responses to SPA, firing at 17.7 [10.0-24.0] % of the events (median [±95% confidence interval]; Fig. 4F, significantly lower than in epileptic tissue, $p<0.05$).

Anatomical examinations

When counting NeuN-immunoreactive neurons, we found slightly lower cell densities in all layers in the epileptic (n=14202 neurons from two patients) than in the non-epileptic (n= 8633 neurons from two patients) neocortex (Fig. 5A, B; Table 8). This is in accordance with previous findings showing that neuron numbers are lower in the epileptic neocortex affected by focal cortical dysplasia compared to the adjacent, non-affected neocortex (Thom *et al.*, 2005). Furthermore, neuron density was slightly higher in all layers in the regions where SPA was generated than in the area where SPA could not be detected, both in specimens from epileptic (SPA: 1820±1338, no SPA: 1694±1244 cell/mm^2) and tumour patients (SPA: 2202±1635, no SPA: 1834±1374 cell/mm^2, Table 8).

To examine the changes of perisomatic inhibition (Del Rio & DeFelipe, 1994), we counted the parvalbumin (PV)-positive interneurons in the human epileptic (n=4) and non-epileptic (n=3) neocortical slices. We determined the density of PV-stained interneurons in

areas with and without SPA of the same slice. Density was very variable when comparing areas generating and areas lacking SPA. We found no correlation between the presence of SPA and the number of PV-stained neurons. The density of PV-positive cells was lower in areas with SPA than in regions without SPA in 3 slices from epileptic and in 2 slices from tumor patients, but it was higher in one and one slice derived from epileptic and tumor patients. On average, PV-positive interneuron density was slightly lower in regions generating SPA than areas lacking SPA in epileptic patients (45.0±11.4 cells/mm^2 in regions with SPA vs. 54.1±19.1 cells/mm^2 in regions without SPA), while it was slightly higher in tumor patients (87.7±26.9 cells/mm^2 in regions with SPA vs. 78.1±14.5 cells/mm^2 in regions without SPA). As previously described (DeFelipe *et al.*, 1993), the overall density of PV-positive cells was significantly lower ($p<0.05$) in epileptic (49.5±15.4 cells/mm^2) than in non-epileptic (82.9±20.0 cells/mm^2) neocortex.

Synaptic reorganization has been found in epileptic tissue for both excitatory and inhibitory networks (Marco & DeFelipe, 1997). We examined the account of this phenomenon on the emergence of SPA by investigating 757 synapses in 5136 μm^2 in epileptic (n=3) and 679 synapses in 6144 μm^2 in tumour (n=3) samples. Asymmetrical (=presumably excitatory) and symmetrical (=presumably inhibitory) synapse numbers per unit area were determined at electron microscopic level. Synapse densities were similar in areas generating and not generating SPA both in epileptic and tumour specimens (Fig. 5C-G, Table 9). Interestingly, the density of inhibitory synapses was not lower, but slightly higher in epileptic (7.9±1.9 symmetrical synapses/100 μm^2) compared to non-epileptic tissue (6.7±1.1 synapses/100 μm^2), as it could have been expected based on the lower numbers of PV-positive cells. Moreover, the density of excitatory synapses and thus, the total synaptic density were significantly higher in epileptic (7.3±2.1 asymmetrical synapses/100 μm^2 and 15.2±3.7

synapses/100 μm^2) than in non-epileptic tissue (4.2±1.0 asymmetrical synapses/100 μm^2 and 10.9±1.8 synapses/100 μm^2, $p<0.0001$).

Discussion

Hyperexcitability in the human epileptic neocortex

The main goal of the present study was to explore how the excess excitation of the epileptic neuronal network contributes to the generation of synchronous population bursts. The spontaneously occurring SPAs served as an excellent model for the synchronous activity of neocortical neural assemblies. We found that the hyperexcitability of the human epileptic neocortex is manifested not only at cellular (for review see Avoli *et al.*, 2005), but also at network level. In the epileptic compared to non-epileptic neocortex, SPAs occurred in a higher proportion of slices, more multiple SPAs were detected, and the LFPg amplitude of SPAs was also higher. The higher percentage of depolarizing cells, discharging more frequently during SPA also demonstrate the hyperexcitability of the epileptic neuronal network (see also McCormick & Contreras, 2001). The increased numbers of excitatory synapses together with a slightly decreased neuronal density confirm the phenomenon of epileptic synaptic reorganization (Marco & DeFelipe, 1997), and provide further evidence for an impaired balance between excitatory and inhibitory signaling in the human neocortex. The decreased number of parvalbumin-positive interneurons (staining perisomatic inhibitory basket and axo-axonic cells) could indicate an impaired inhibition in the epileptic neocortex (see also DeFelipe *et al.*, 1993). However, when we investigated the density of inhibitory synapses independent of their parvalbumin, contrary to a previous study (Marco & DeFelipe, 1997), we did not observe any loss, but a slightly increased number of inhibitory connections in the epileptic neocortex. This suggest that inhibitory circuits might also participate in the epileptic synaptic reorganization, as they do in the human hippocampus (Wittner *et al.*, 2001).

High frequency oscillations were detected in the human neocortex during both normal and epileptic brain states (Blanco *et al.*, 2010), and increased ripples and fast ripples were

proposed to identify the epileptogenic zone (Worrell *et al.*, 2008; Jacobs *et al.*, 2012). Since in vitro slice preparations represent considerably altered conditions compared to in vivo human neocortical circuitry, solid conclusions cannot be made on the presence of high frequency oscillations. However, the same tendency could be observed in our samples as in vivo, i.e. higher numbers of SPAs and IIDs were associated with prominent HFOs in epileptic vs. tumour tissue. In addition, the HFO power of IIDs was about twice as large compared to that of SPAs, supporting the hypersynchronous nature of epileptic processes.

Our observations indicate that the emergence of population activity is related to the level of excitation and synchrony in the human neocortex, although both glutamatergic and GABAergic signaling participate in it (see pharmacological results). The generation of SPAs in epileptic samples is linked to a higher degree of excitation compared to non-epileptic tissue. The sprouting of excitatory connections, as well as the higher numbers of depolarizing and more reliably firing cells contribute to the modification of the neocortical neuronal network, and seems to facilitate the emergence of SPAs (more slices exhibit SPA, more multiple SPAs). The emergence of IIDs is associated with an even more elevated level of excitation and synchrony, reflected in the significantly higher values of LFPg, MUA and HFO power values. Future studies are needed to define (if possible) the subtle border between physiological and pathological processes.

Complexity of the human neocortex

As in a recent study (Mohan *et al.*, 2015), we found that the total dendritic length of human neocortical pyramidal cells (~34 mm) is over three times as large as that of rodents (~9 to 10 mm; (Ascoli *et al.*, 2007; Krieger *et al.*, 2007; Chen *et al.*, 2014). The exceptionally long dendritic tree of human neurons offers the possibility of receiving input from a very large number of synapses, and thus, may serve as the anatomical basis of the highly interconnected

and reliable neocortical circuitry (Molnár *et al.*, 2008). Human neocortical neurons show heterogeneous firing patterns during interictal spikes (Keller *et al.*, 2010), supporting the complexity of distinct neuronal groups interacting to generate hypersynchronous discharges. The occurrence of multiple SPAs and simultaneous SPAs-IIDs in the same slice also indicate the presence of an exceptionally complex neuronal network able to induce different types of synchronies. Our results provide further evidence that the anatomical and physiological complexity of the human neocortex seems to highly exceed that of rodents. The ability of the neocortical neuronal network to spontaneously generate complex synchronies may contribute to cognitive functions characteristic to humans. The complexity of the neuronal circuit provides the potential of improved encoding capabilities (Fourcaud-Trocme *et al.*, 2003; Ilin *et al.*, 2013; Eyal *et al.*, 2014), which might have resulted in an evolutionary benefit for humans.

Two distinct types of synchronies generated by human neocortical slices

In the present study, we show that two types of spontaneous synchronous activities can emerge in human neocortical slice preparations. The initiation layers, occurrence rate and network characteristics provided a clear distinction between IIDs and SPAs.

In our records, spontaneous IIDs were generated only in slices from epileptic patients, mainly in the granular or infragranular layers, like in vivo interictal spikes (Ulbert *et al.*, 2004a). The recurrence frequency of IIDs was ~0.05 Hz, a value comparable to the 4-amino-pyridine induced epileptiform activity recorded in human neocortical slices (0.3 to 0.1 Hz; (Avoli *et al.*, 1994) and to spiking activity in the subiculum (~0.15 Hz) of epileptic patients (Fabó *et al.*, 2008). The large LFPg transient, the initial current sink and the considerably enhanced cell firing recalled the characteristics of interictal spikes detected in vivo (Ulbert *et al.*, 2004a; Fabó *et al.*, 2008), and those of the Mg^{2+}-free model of epileptic activity recorded

in the human neocortex in vitro (Avoli *et al.*, 1995). The remarkably high ripple and fast ripple powers during IIDs further indicate the hypersynchronous nature of these bursts. The striking similarity of IIDs to in vivo interictal spikes and to pharmacologically induced epileptiform events recorded in human slices suggest that this activity might be linked to epileptic processes. The fact that they could be recorded only in specimens originating from epileptic patients further supports this idea.

SPAs described in our samples were significantly different from IIDs, and showed remarkable similarities to population activity recorded in epileptic human hippocampal (Cohen *et al.*, 2002; Wozny *et al.*, 2005; Huberfeld *et al.*, 2007; Wittner *et al.*, 2009) and neocortical (Köhling *et al.*, 1998; Roopun *et al.*, 2010; Pallud *et al.*, 2014) slices. The cellular responses of our intracellularly recorded neurons were also comparable to intracellular reflections of spontaneous network activity detected in human neocortical neurons (Schwartzkroin & Knowles, 1984; Schwartzkroin & Haglund, 1986). SPAs were recorded in slices derived from epileptic patients and from tumour patients with no preoperative clinical or electrographic manifestations of epileptic activity. Contrary to IIDs, SPAs were initiated mainly in the supragranular layers (see also Köhling *et al.*, 1998; Pallud *et al.*, 2014), and their recurrence frequency was one order of magnitude higher than that of IIDs. They were also characterized by a field potential transient with superimposed high frequency oscillations and increased cellular activity. However, all examined network properties (LFPg, CSD, MUA, high frequency oscillation power) gave significantly lower values compared to IIDs, suggesting that considerably lower numbers of neurons participate in these synchronous events.

Epileptic activity in human tissue, in vitro?

The question whether human cortical tissue retains its epileptic activity has been investigated since the first in vitro human studies (in 1970's, for review see Avoli *et al.*, 2005). Spontaneous interictal-like activity was very rarely observed, whereas ictal-like activity could be never reported in human preparations, even in tissue derived from brain regions chronically involved in seizure activity. However, both interictal and ictal-like activities could be induced by appropriate pharmacological agents. The most obvious conclusions of these work were that deafferentation might be linked to the disappearance of epileptic activity, or that foci of epileptic activity are small, and thus difficult to detect (Köhling *et al.*, 1998). The size of the tissue sample – and thus, the number of cells constituting the neuronal network – has been related to the emergence of synchronous activity in the rodent hippocampus (Wu *et al.*, 2005), suggesting that a minimal number of neurons and connections (Wittner & Miles, 2007) are required to generate synchronous activity. A systematic study would be needed to reveal what is the smallest subset of a human cortical network which can retain its spontaneous epileptic activity. The knowledge about the differences in neuron/glia numbers, in synaptic connectivity, differences in receptor/transmitter systems in the epileptic cortex compared to non-epileptic samples would also help to make an estimation about the smallest tissue sample able to generate epileptic activity in vitro.

The epileptogenicity of the in vitro spontaneous network events is a debated question since the beginning of human in vitro research. The picture is notably complex when regarding different species and different cortical regions. Since healthy human samples are not available, researchers often use animal tissue as control. In vitro spontaneous neocortical network events could be detected neither in healthy rodents (Köhling *et al.*, 1998; Avoli *et al.*, 2005), nor in primates (Schwartzkroin & Haglund, 1986). Complex population bursts could, however, be evoked in neocortical slices derived from non-epileptic patients by activating

single pyramidal cells (Molnár *et al.*, 2008). Population activity arising in healthy monkey hippocampal slices was also considered to be proof that spontaneous synchronous bursts are not related to epilepsy (Schwartzkroin & Haglund, 1986). Accordingly, in the last two decades, work exploring the spontaneous network activity in the hippocampus of healthy rodents consistently correlated this type of events to sharp-wave ripple complexes – the physiologically occurring phenomenon thought to participate in learning and memory consolidation processes (for review see Buzsáki, 2015). On the other hand, the behavior of human neocortical neurons (Prince & Wong, 1981; Schwartzkroin & Knowles, 1984; Strowbridge *et al.*, 1992; Avoli *et al.*, 2003; Williamson *et al.*, 2003), and the similarities in the wave form of in vitro events and in vivo interictal spikes (Cohen *et al.*, 2002; Pallud *et al.*, 2014) strengthened the idea that in vitro population bursts are linked to epilepsy. Neocortical population events were either compared to sharp waves – the clinical term for the short variant of interictal discharges (Köhling *et al.*, 1998; Köhling *et al.*, 1999), or were called interictal-like activity (Pallud *et al.*, 2014). In the latter study network events were recorded in neocortical slices from tumour patients both with or without preoperative seizures. The patients suffered from gliomas known to be highly epileptogenic, and the authors related the emergence of these events to the epileptogenicity of the human peritumoural neocortex. In summary, some studies indicate that in vitro population activity is not related to epileptic processes (Schwartzkroin & Haglund, 1986; Molnár *et al.*, 2008; Szegedi *et al.*, 2016), whereas most authors believe in its epileptiform nature (Prince & Wong, 1981; Schwartzkroin & Knowles, 1984; Strowbridge *et al.*, 1992; Köhling *et al.*, 1998; Cohen *et al.*, 2002; Avoli *et al.*, 2003; Williamson *et al.*, 2003; Pallud *et al.*, 2014).

Our results strongly support the hypothesis that SPAs are not a direct reflection of neocortical epileptogenicity. SPAs detected in slices derived from tumour patients without having preoperative clinical and electrographic manifestations of epileptic seizures were very

similar in all aspects to those recorded from tissue resected from epileptic patients. Furthermore, the higher neuronal density in the spots generating SPA also indicates its non-pathological feature, since focal cortical epilepsies are linked to neuron loss (Thom *et al.*, 2005). However, signs of epileptic hyperexcitability can be observed in human epileptic neocortical slices, since they can generate IIDs as well, a presumably epileptiform synchronous activity.

Acknowledgement

The authors are thankful to Ms. K. Lengyel, E. Szépné Simon and Mr. Gy. Goda for technical assistance, and for Dr. Richard Miles for his helpful comments.

Author contributions

Kinga Tóth performed data acquisition and analysis (anatomy and electrophysiology), Katharina T. Hofer performed data acquisition, analysis and contributed to the design of the study (electrophysiology), Ágnes Kandrács performed data acquisition and analysis (electrophysiology), László Entz provided neurological data and human tissue, Attila Bagó provided human tissue, Loránd Erőss provided neurological data and human tissue, Zsófia Jordán provided neurological data, Gábor Nagy provided human tissue, András Sólyom provided neurological data, Dániel Fabó provided neurological data, and made the design of the study, István Ulbert made the conception, the design of the study, wrote the article and Lucia Wittner made the design of the study, collected and analyzed data (anatomy, electrophysiology), and wrote the article.

Competing Interests

None of the authors has any conflict of interest.

Ethical approval

All procedures performed in this study involving human participants were in accordance with the ethical standards of the institutional and national research committees

and with the 1964 Helsinki declaration and its later amendments or comparable ethical standards.

Funding

This study was supported by the Postdoctoral fellowship of the Hungarian Academy of Sciences (to K. T.), by the Hungarian Brain Research Program - Grants No. KTIA_13_NAP-A-IV/1-4,6 and KTIA 13 NAP-A-I/1 (to I. U.) and KTIA_NAP_13-1-2013-0001 (to D. F.); by the EU FP7 Grant No. 600925 NeuroSeeker, and by the Hungarian National Research Fund OTKA K119443 (to L. W.) and PD121123 (to K. T.) grants.

References

Alonso-Nanclares L, Garbelli R, Sola RG, Pastor J, Tassi L, Spreafico R & DeFelipe J. (2005). Microanatomy of the dysplastic neocortex from epileptic patients. *Brain* **128,** 158-173.

Ascoli GA, Donohue DE & Halavi M. (2007). NeuroMorpho.Org: a central resource for neuronal morphologies. *J Neurosci* **27,** 9247-9251.

Avoli M, Louvel J, Drapeau C, Pumain R & Kurcewicz I. (1995). GABAA-mediated inhibition and in vitro epileptogenesis in the human neocortex. *J Neurophysiol* **73,** 468-484.

Avoli M, Louvel J, Mattia D, Olivier A, Esposito V, Pumain R & D'Antuono M. (2003). Epileptiform synchronization in the human dysplastic cortex. *Epileptic Disord* **5 Suppl 2,** S45-50.

Avoli M, Louvel J, Pumain R & Köhling R. (2005). Cellular and molecular mechanisms of epilepsy in the human brain. *Prog Neurobiol* **77,** 166-200.

Avoli M, Mattia D, Siniscalchi A, Perreault P & Tomaiuolo F. (1994). Pharmacology and electrophysiology of a synchronous GABA-mediated potential in the human neocortex. *Neuroscience* **62,** 655-666.

Avoli M & Olivier A. (1989). Electrophysiological properties and synaptic responses in the deep layers of the human epileptogenic neocortex in vitro. *J Neurophysiol* **61,** 589-606.

Blanco JA, Stead M, Krieger A, Viventi J, Marsh WR, Lee KH, Worrell GA & Litt B. (2010). Unsupervised classification of high-frequency oscillations in human neocortical epilepsy and control patients. *J Neurophysiol* **104,** 2900-2912.

Bragin A, Engel J, Jr., Wilson CL, Fried I & Buzsáki G. (1999). High-frequency oscillations in human brain. *Hippocampus* **9,** 137-142.

Buzsáki G. (2015). Hippocampal sharp wave-ripple: A cognitive biomarker for episodic memory and planning. *Hippocampus* **25,** 1073-1188.

Chen JR, Wang BN, Tseng GF, Wang YJ, Huang YS & Wang TJ. (2014). Morphological changes of cortical pyramidal neurons in hepatic encephalopathy. *BMC Neurosci* **15,** 15.

Cohen I, Navarro V, Clémenceau S, Baulac M & Miles R. (2002). On the origin of interictal activity in human temporal lobe epilepsy in vitro. *Science* **298,** 1418-1421.

de Curtis M & Avanzini G. (2001). Interictal spikes in focal epileptogenesis. *Prog Neurobiol* **63,** 541-567.

DeFelipe J, Garcia Sola R, Marco P, del Rio MR, Pulido P & Ramon y Cajal S. (1993). Selective changes in the microorganization of the human epileptogenic neocortex revealed by parvalbumin immunoreactivity. *Cereb Cortex* **3,** 39-48.

Del Rio MR & DeFelipe J. (1994). A study of SMI 32-stained pyramidal cells, parvalbumin-immunoreactive chandelier cells, and presumptive thalamocortical axons in the human temporal neocortex. *J Comp Neurol* **342,** 389-408.

Eyal G, Mansvelder HD, de Kock CP & Segev I. (2014). Dendrites impact the encoding capabilities of the axon. *J Neurosci* **34,** 8063-8071.

Fabó D, Maglóczky Z, Wittner L, Pék A, Erőss L, Czirják S, Vajda J, Sólyom A, Rásonyi G, Szűcs A, Kelemen A, Juhos V, Grand L, Dombovári B, Halász P, Freund TF, Halgren E, Karmos G & Ulbert I. (2008). Properties of in vivo interictal spike generation in the human subiculum. *Brain* **131,** 485-499.

Fourcaud-Trocme N, Hansel D, van Vreeswijk C & Brunel N. (2003). How spike generation mechanisms determine the neuronal response to fluctuating inputs. *J Neurosci* **23,** 11628-11640.

Gabriel S, Njunting M, Pomper JK, Merschhemke M, Sanabria ER, Eilers A, Kivi A, Zeller M, Meencke HJ, Cavalheiro EA, Heinemann U & Lehmann TN. (2004). Stimulus and potassium-induced epileptiform activity in the human dentate gyrus from patients with and without hippocampal sclerosis. *J Neurosci* **24,** 10416-10430.

Gorji A, Hohling JM, Madeja M, Straub H, Kohling R, Tuxhorn I, Ebner A, Wolf P, Panneck HW, Behne F, Lahl R & Speckmann EJ. (2002). Effect of levetiracetam on epileptiform discharges in human neocortical slices. *Epilepsia* **43,** 1480-1487.

Gulyás AI, Szabó GG, Ulbert I, Holderith N, Monyer H, Erdélyi F, Szabó G, Freund TF & Hájos N. (2010). Parvalbumin-containing fast-spiking basket cells generate the field potential oscillations induced by cholinergic receptor activation in the hippocampus. *J Neurosci* **30,** 15134-15145.

Hájos N, Karlócai MR, Németh B, Ulbert I, Monyer H, Szabó G, Erdélyi F, Freund TF & Gulyás AI. (2013). Input-output features of anatomically identified CA3 neurons during hippocampal sharp wave/ripple oscillation in vitro. *J Neurosci* **33,** 11677-11691.

Heinemann U, Gabriel S, Jauch R, Schulze K, Kivi A, Eilers A, Kovacs R & Lehmann TN. (2000). Alterations of glial cell function in temporal lobe epilepsy. *Epilepsia* **41,** S185-189.

Hofer KT, Kandrács A, Ulbert I, Pál I, Szabó C, Héja L & Wittner L. (2015). The hippocampal CA3 region can generate two distinct types of sharp wave-ripple complexes, in vitro. *Hippocampus* **25,** 169-186.

Huberfeld G, Menendez de la Prida L, Pallud J, Cohen I, Le Van Quyen M, Adam C, Clémenceau S, Baulac M & Miles R. (2011). Glutamatergic pre-ictal discharges emerge at the transition to seizure in human epilepsy. *Nat Neurosci* **14,** 627-634.

Huberfeld G, Wittner L, Clémenceau S, Baulac M, Kaila K, Miles R & Rivera C. (2007). Perturbed chloride homeostasis and GABAergic signaling in human temporal lobe epilepsy. *J Neurosci* **27,** 9866-9873.

Ilin V, Malyshev A, Wolf F & Volgushev M. (2013). Fast computations in cortical ensembles require rapid initiation of action potentials. *J Neurosci* **33,** 2281-2292.

Isokawa M & Fried I. (1996). Extracellular slow negative transient in the dentate gyrus of human epileptic hippocampus in vitro. *Neuroscience* **72,** 31-37.

Jacobs J, Staba R, Asano E, Otsubo H, Wu JY, Zijlmans M, Mohamed I, Kahane P, Dubeau F, Navarro V & Gotman J. (2012). High-frequency oscillations (HFOs) in clinical epilepsy. *Prog Neurobiol* **98,** 302-315.

Keller CJ, Truccolo W, Gale JT, Eskandar E, Thesen T, Carlson C, Devinsky O, Kuzniecky R, Doyle WK, Madsen JR, Schomer DL, Mehta AD, Brown EN, Hochberg LR, Ulbert I, Halgren E & Cash SS. (2010). Heterogeneous neuronal firing patterns during interictal epileptiform discharges in the human cortex. *Brain* **133,** 1668-1681.

Kivi A, Lehmann TN, Kovacs R, Eilers A, Jauch R, Meencke HJ, von Deimling A, Heinemann U & Gabriel S. (2000). Effects of barium on stimulus-induced rises of [K+]o in human epileptic non-sclerotic and sclerotic hippocampal area CA1. *Eur J Neurosci* **12,** 2039-2048.

Köhling R, Lucke A, Straub H, Speckmann EJ, Tuxhorn I, Wolf P, Pannek H & Oppel F. (1998). Spontaneous sharp waves in human neocortical slices excised from epileptic patients. *Brain* **121 (Pt 6),** 1073-1087.

Köhling R, Qu M, Zilles K & Speckmann EJ. (1999). Current-source-density profiles associated with sharp waves in human epileptic neocortical tissue. *Neuroscience* **94,** 1039-1050.

Krieger P, Kuner T & Sakmann B. (2007). Synaptic connections between layer 5B pyramidal neurons in mouse somatosensory cortex are independent of apical dendrite bundling. *J Neurosci* **27,** 11473-11482.

Lehmann TN, Gabriel S, Kovacs R, Eilers A, Kivi A, Schulze K, Lanksch WR, Meencke HJ & Heinemann U. (2000). Alterations of neuronal connectivity in area CA1 of hippocampal slices from temporal lobe epilepsy patients and from pilocarpine-treated epileptic rats. *Epilepsia* **41,** S190-194.

Marco P & DeFelipe J. (1997). Altered synaptic circuitry in the human temporal neocortex removed from epileptic patients. *Exp Brain Res* **114,** 1-10.

McCormick DA. (1989). GABA as an inhibitory neurotransmitter in human cerebral cortex. *J Neurophysiol* **62,** 1018-1027.

McCormick DA & Contreras D. (2001). On the cellular and network bases of epileptic seizures. *Annu Rev Physiol* **63,** 815-846.

Mohan H, Verhoog MB, Doreswamy KK, Eyal G, Aardse R, Lodder BN, Goriounova NA, Asamoah B, AB BB, Groot C, van der Sluis S, Testa-Silva G, Obermayer J, Boudewijns ZS, Narayanan RT, Baayen JC, Segev I, Mansvelder HD & de Kock CP. (2015). Dendritic and Axonal Architecture of Individual Pyramidal Neurons across Layers of Adult Human Neocortex. *Cereb Cortex* **25,** 4839-4853.

Molnár G, Oláh S, Komlósi G, Füle M, Szabadics J, Varga C, Barzó P & Tamás G. (2008). Complex events initiated by individual spikes in the human cerebral cortex. *PLoS Biol* **6,** e222.

Pallud J, Le Van Quyen M, Bielle F, Pellegrino C, Varlet P, Labussiere M, Cresto N, Dieme MJ, Baulac M, Duyckaerts C, Kourdougli N, Chazal G, Devaux B, Rivera C, Miles R, Capelle L & Huberfeld G. (2014). Cortical GABAergic excitation contributes to epileptic activities around human glioma. *Science translational medicine* **6,** 244ra289.

Papatheodoropoulos C & Kostopoulos G. (2002). Spontaneous, low frequency (approximately 2-3 Hz) field activity generated in rat ventral hippocampal slices perfused with normal medium. *Brain Res Bull* **57,** 187-193.

Prince DA & Wong RK. (1981). Human epileptic neurons studied in vitro. *Brain Res* **210,** 323-333.

Roopun AK, Simonotto JD, Pierce ML, Jenkins A, Nicholson C, Schofield IS, Whittaker RG, Kaiser M, Whittington MA, Traub RD & Cunningham MO. (2010). A nonsynaptic mechanism underlying interictal discharges in human epileptic neocortex. *Proc Natl Acad Sci U S A* **107,** 338-343.

Schwartzkroin PA & Haglund MM. (1986). Spontaneous rhythmic synchronous activity in epileptic human and normal monkey temporal lobe. *Epilepsia* **27,** 523-533.

Schwartzkroin PA & Knowles WD. (1984). Intracellular study of human epileptic cortex: in vitro maintenance of epileptiform activity? *Science* **223,** 709-712.

Simon A, Traub RD, Vladimirov N, Jenkins A, Nicholson C, Whittaker RG, Schofield I, Clowry GJ, Cunningham MO & Whittington MA. (2014). Gap junction networks can generate both ripple-like and fast ripple-like oscillations. *Eur J Neurosci* **39,** 46-60.

Strowbridge BW, Masukawa LM, Spencer DD & Shepherd GM. (1992). Hyperexcitability associated with localizable lesions in epileptic patients. *Brain Res* **587,** 158-163.

Szegedi V, Paizs M, Csákvári E, Molnár G, Barzó P, Tamás G & Lamsa K. (2016). Plasticity in Single Axon Glutamatergic Connection to GABAergic Interneurons Regulates Complex Events in the Human Neocortex. *PLoS Biol* **14,** e2000237.

Thom M, Martinian L, Sen A, Cross JH, Harding BN & Sisodiya SM. (2005). Cortical neuronal densities and lamination in focal cortical dysplasia. *Acta neuropathologica* **110,** 383-392.

Tóth K, Erőss L, Vajda J, Halász P, Freund TF & Maglóczky Z. (2010). Loss and reorganization of calretinin-containing interneurons in the epileptic human hippocampus. *Brain* **133,** 2763-2777.

Ulbert I, Halgren E, Heit G & Karmos G. (2001). Multiple microelectrode-recording system for human intracortical applications. *J Neurosci Methods* **106,** 69-79.

Ulbert I, Heit G, Madsen J, Karmos G & Halgren E. (2004a). Laminar analysis of human neocortical interictal spike generation and propagation: current source density and multiunit analysis in vivo. *Epilepsia* **45 Suppl 4,** 48-56.

Ulbert I, Maglóczky Z, Erőss L, Czirják S, Vajda J, Bognár L, Tóth S, Szabó Z, Halász P, Fabó D, Halgren E, Freund TF & Karmos G. (2004b). In vivo laminar electrophysiology co-registered with histology in the hippocampus of patients with temporal lobe epilepsy. *Exp Neurol* **187,** 310-318.

Williamson A, Patrylo PR, Lee S & Spencer DD. (2003). Physiology of human cortical neurons adjacent to cavernous malformations and tumors. *Epilepsia* **44,** 1413-1419.

Williamson A, Patrylo PR, Pan J, Spencer DD & Hetherington H. (2005). Correlations between granule cell physiology and bioenergetics in human temporal lobe epilepsy. *Brain* **128,** 1199-1208.

Wittner L, Huberfeld G, Clémenceau S, Erőss L, Dezamis E, Entz L, Ulbert I, Baulac M, Freund TF, Maglóczky Z & Miles R. (2009). The epileptic human hippocampal cornu ammonis 2 region generates spontaneous interictal-like activity in vitro. *Brain* **132,** 3032-3046.

Wittner L, Maglóczky Z, Borhegyi Z, Halász P, Tóth S, Erőss L, Szabó Z & Freund TF. (2001). Preservation of perisomatic inhibitory input of granule cells in the epileptic human dentate gyrus. *Neuroscience* **108,** 587-600.

Wittner L & Miles R. (2007). Factors defining a pacemaker region for synchrony in the hippocampus. *J Physiol* **584,** 867-883.

Worrell GA, Gardner AB, Stead SM, Hu S, Goerss S, Cascino GJ, Meyer FB, Marsh R & Litt B. (2008). High-frequency oscillations in human temporal lobe: simultaneous microwire and clinical macroelectrode recordings. *Brain* **131,** 928-937.

Wozny C, Knopp A, Lehmann TN, Heinemann U & Behr J. (2005). The subiculum: a potential site of ictogenesis in human temporal lobe epilepsy. *Epilepsia* **46 Suppl 5,** 17-21.

Wu C, Luk WP, Gillis J, Skinner F & Zhang L. (2005). Size does matter: generation of intrinsic network rhythms in thick mouse hippocampal slices. *J Neurophysiol* **93,** 2302-2317.

Figure legend

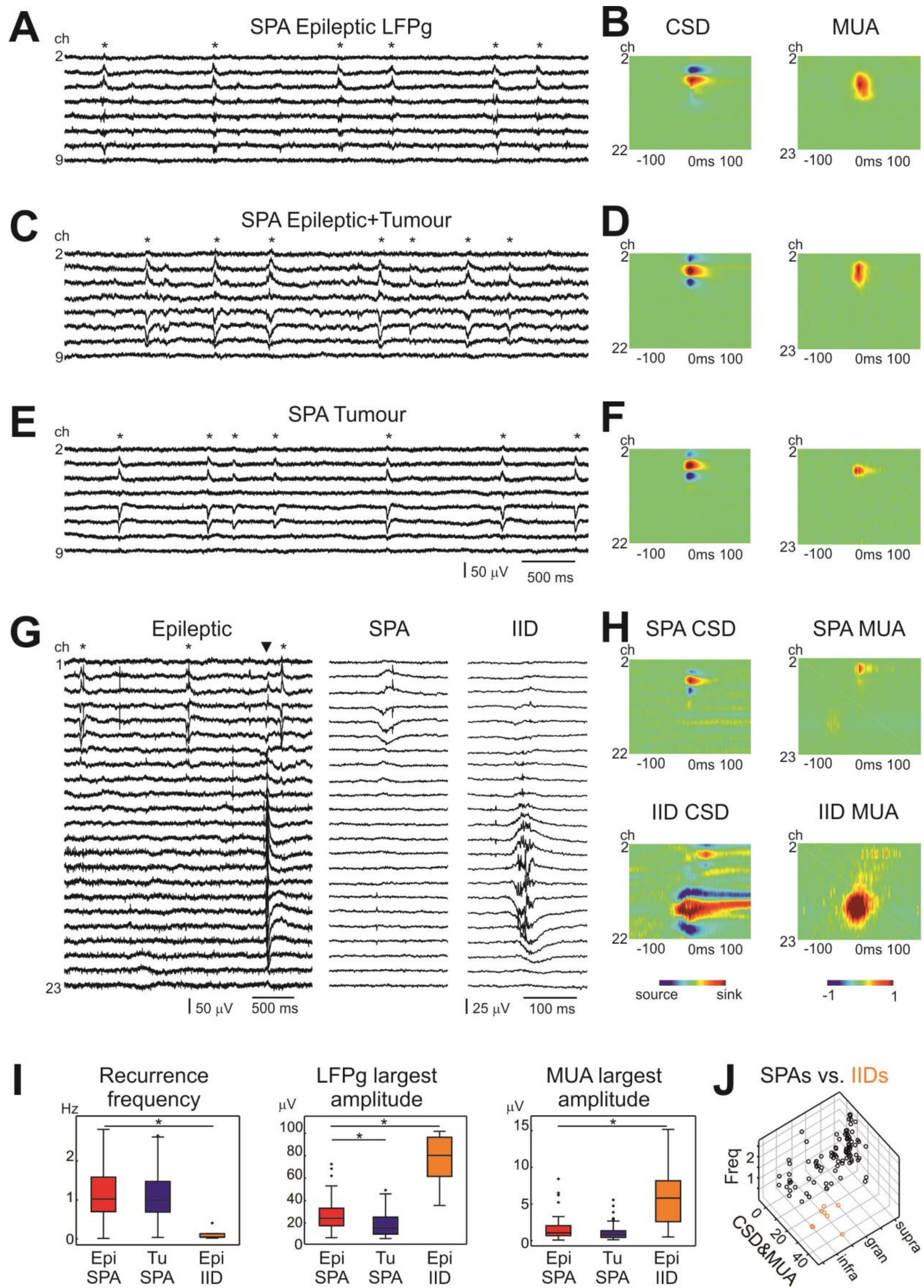

Figure 1.

Network characteristics of SPAs in human neocortical slices.

SPAs were observed in tissue from epileptic patients without tumour (A-B), epileptic patients with tumour (C-D) and tumour patients without epilepsy (E-F). Furthermore, IID was detected in the epileptic neocortex (G-H). Left panels show LFPg traces from eight (A, C, E) channels positioned in the supragranular layers, while (G) shows 23 channels covering the entire width of the neocortex, with simultaneously occurring SPA and IID. Asterisks label SPA events (A, C, E, G), the triangle (G) indicates the IID event. One SPA and IID event each is magnified on the right side (G). Color maps (B, D, F, H) show the CSD and the change in MUA. In most SPA cases CSD consisted of a pair or triple of simultaneous sinks and sources and were similar in all three patient groups. Warm colors depict sinks, while cold colors indicate sources. MUA increase was detected during SPAs and IIDs in almost all cases. Warm colors show MUA increase, cold colors label MUA decrease. Note the higher amplitude of CSD and MUA in case of IIDs (color scales are the same for all heat maps).

(I) The recurrence frequency and the MUA were similar for SPAs of epileptic and tumour patients. The LFPg amplitudes were significantly larger for SPAs in epileptic patients than in tumour patients (LFPg: $p<0.01$). All of these network characteristics of IIDs were significantly different from SPAs detected in epileptic tissue ($p<0.01$). * labels significant difference

(J) The values of recurrence frequency (Freq), the average of CSD and MUA (CSD&MUA), and the intracortical location of all SPAs (black circles) and IIDs (orange circles) from epileptic and tumour tissue are shown on a three-dimensional plot.

Epi: epileptic, Tu: tumour, supra: supragranular, gran: granular, infra: infragranular

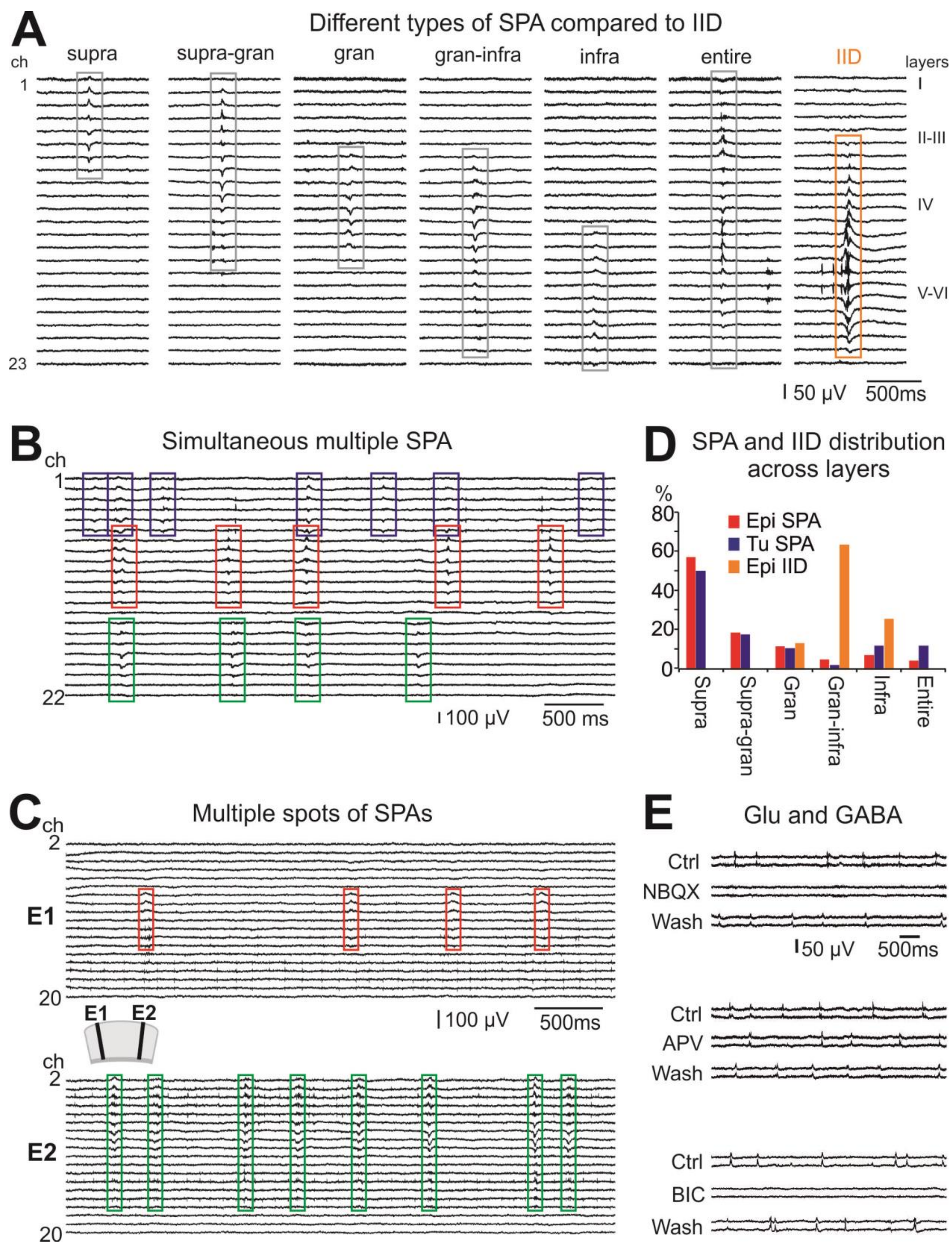

Figure 2

Different types of single and multiple SPAs.

(A) Different types of SPAs were separated based on their location and extension across the neocortical layers. SPAs were found to be spread over supragranular (supra), supragranular+granular (supra-gran), granular (gran), granular+infragranular (gran-infra) or infragranular (infra) layers or over the entire width of the neocortex (entire). For comparison, an IID event is also shown.

Multiple SPAs occurred more frequently in samples from epileptic and epileptic+tumour patients. We differentiated between simultaneous multiple SPAs at one recording site (B) and multiple spots of SPAs in the same slice (C).

(D) The prevalence of the different SPA types was similar in the epileptic and tumour patient groups. Most of the SPAs were generated in the supragranular layers, whereas IIDs emerged mainly in the deeper layers.

(E) The AMPA/kainate type glutamate receptor antagonist NBQX blocks the emergence of SPAs (upper panel). The NMDA type glutamate receptor antagonist DL-APV reduced the frequency of SPAs (middle panel). The GABAA receptor antagonist bicuculline also blocked the generation of SPAs (lower panel). All these effects were reversible.

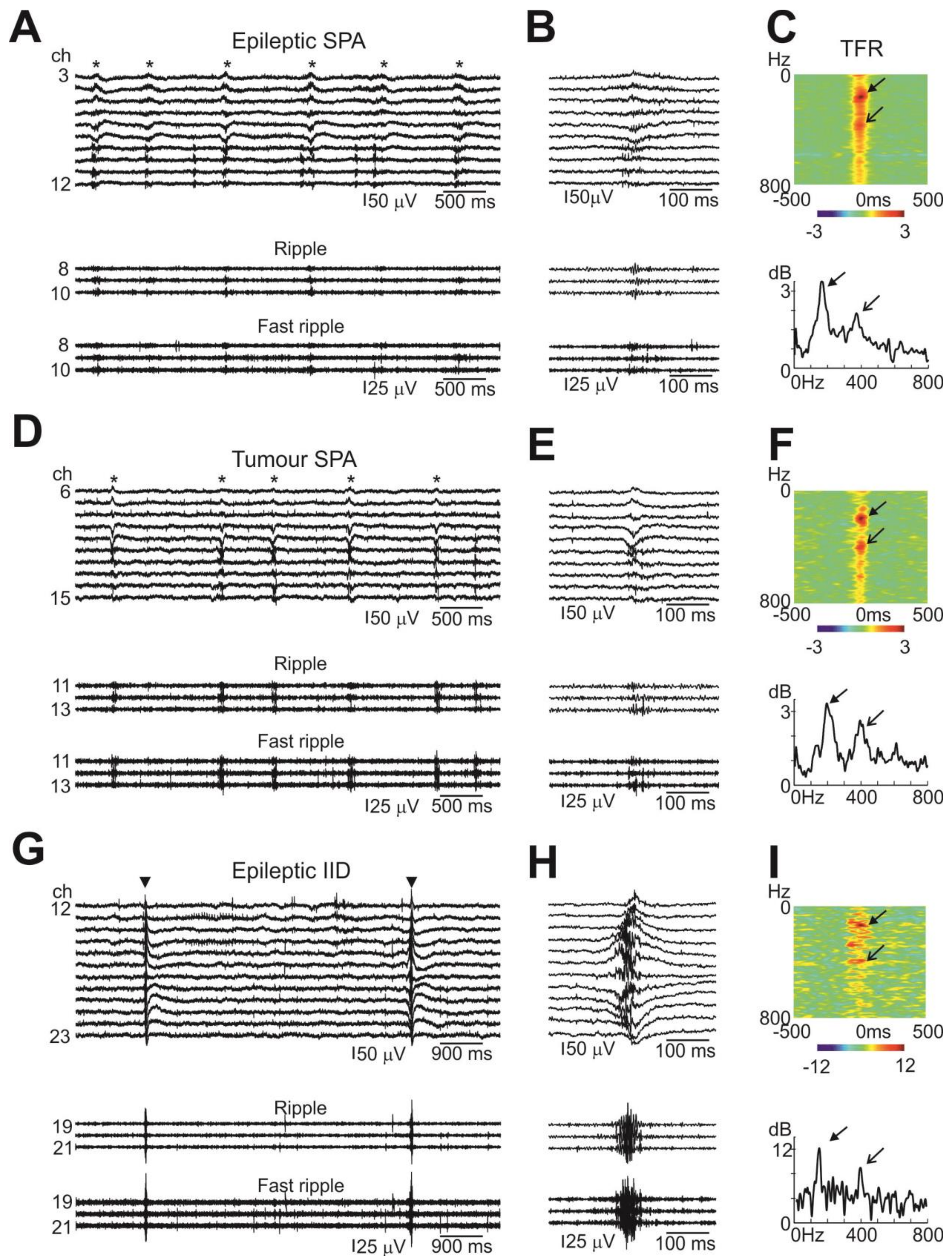

Figure 3

High frequency oscillations during SPAs.

SPAs were more often accompanied by high frequency oscillations in epileptic (A-C) than in tumour (D-F) patients. High frequency oscillations were superimposed on IIDs (G-I) at similar ratios as on epileptic SPAs. Traces in both ripple (A-B, D-E, G-H middle trace) and fast ripple frequency band (A-B, D-E, G-H bottom trace) showed an increased activity during SPAs (asterisks on A, D, upper trace) and IIDs (triangles on G, upper trace). (B) and (E) show one magnified SPA event, (H) shows one IID event. Note the difference in the amplitude of high frequency oscillations between SPAs and IID.

Arrows indicate peaks at ripple frequency, open end arrows mark the peaks at fast ripple frequency on the heat maps (C, F, I, upper panels) and on the line plots made at the LFPg peak (at time 0, lower panels) generated using wavelet analysis (C, F, I, lower panels). Time frequency analysis (TFR, C, F, I) shows the results obtained on channel 10 (A-B), channel 13 (D-E), and channel 19 (G-H), respectively. Warm colors depict an increase in frequency power, cold colors show a decrease. Note the scale differences between TFR plots.

A, D: * labels the SPA events, G: triangle shows IID events

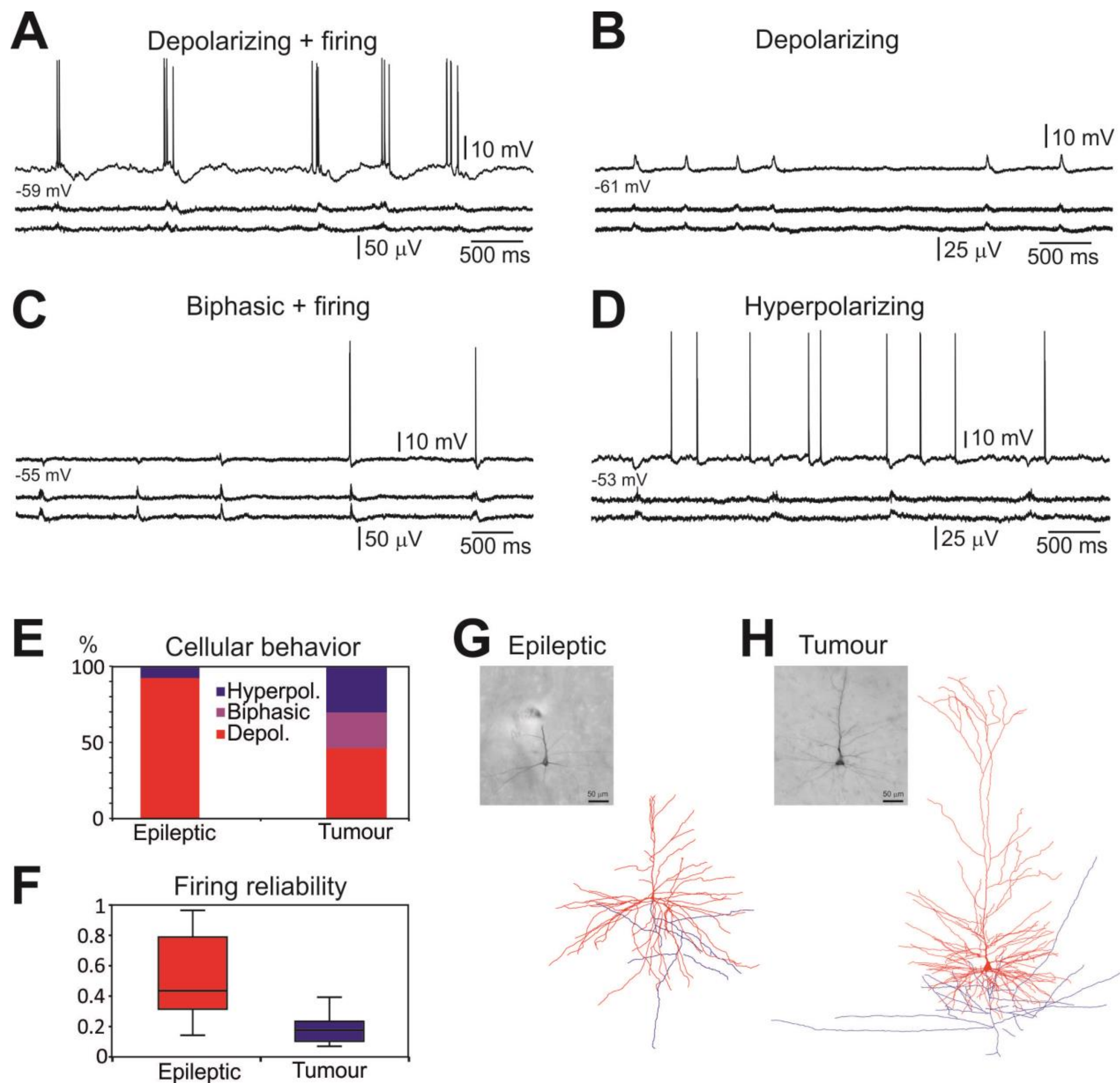

Figure 4

Cellular responses of intracellularly recorded cells.

Human neocortical pyramidal cells showed various behaviors during SPAs (two lower traces) in intracellular records (upper trace): depolarizing (A-B), biphasic (C) or hyperpolarizing (D). In epileptic tissue, seven out of 11 depolarizing cells were also discharging (A) during SPA. In tumour tissue, four out of six depolarizing and all three biphasic cells (C) were also firing during SPA, although with significantly lower reliability (F) than neurons from epileptic tissue ($p<0.05$). (E) The ratio of depolarizing cells was significantly higher in epileptic tissue ($p<0.05$), and biphasic cells were only found in tumour tissue. Light micrographs and three-

dimensional reconstructions show a layer V pyramidal cell from epileptic tissue (G) and a layer II pyramidal cell from tumour tissue (H). Note the very complex dendritic arborization (red) of human cells, and the truncated apical dendrite of the cell in (G). Axons are shown in blue. The same scale bar applies to the micrograph and the reconstruction.

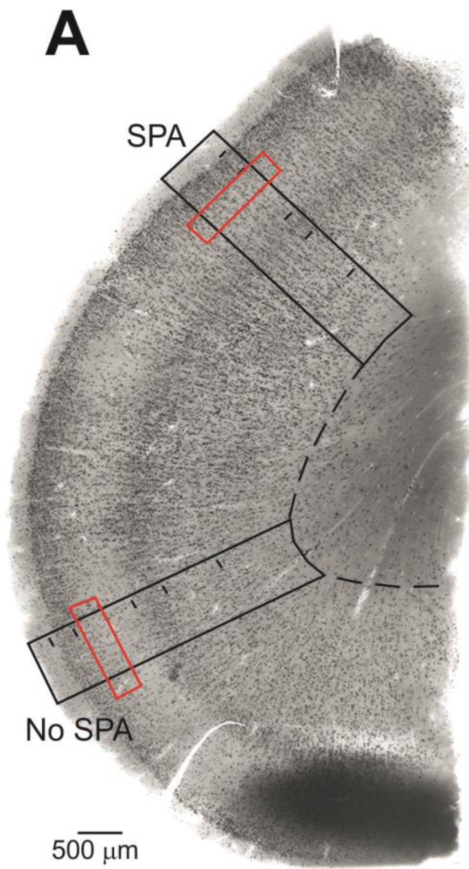
A
SPA
No SPA
500 μm

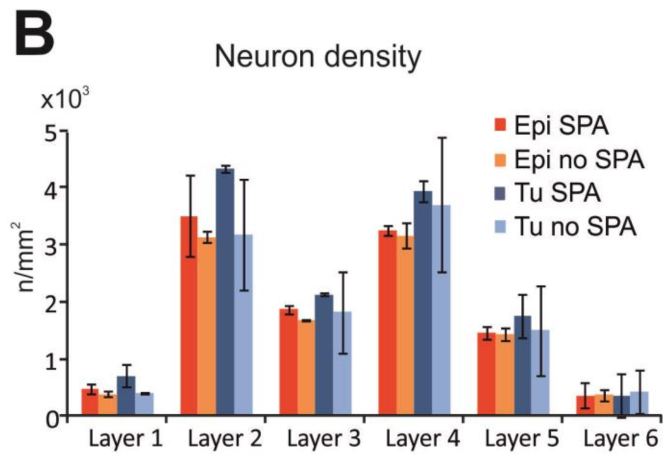
B
Neuron density
x10^3
n/mm^2
Epi SPA
Epi no SPA
Tu SPA
Tu no SPA
Layer 1
Layer 2
Layer 3
Layer 4
Layer 5
Layer 6

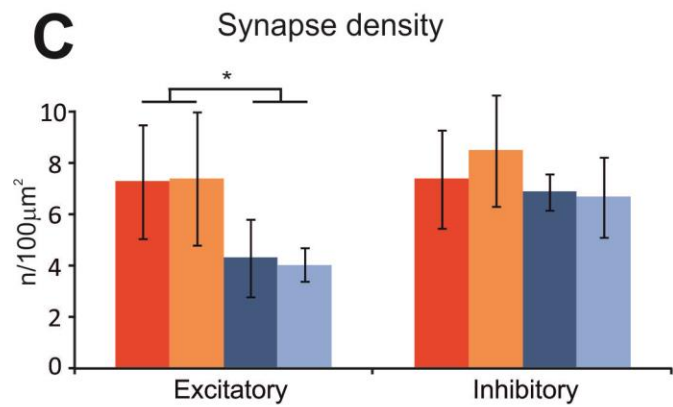
C
Synapse density
n/100μm^2
*
Excitatory
Inhibitory

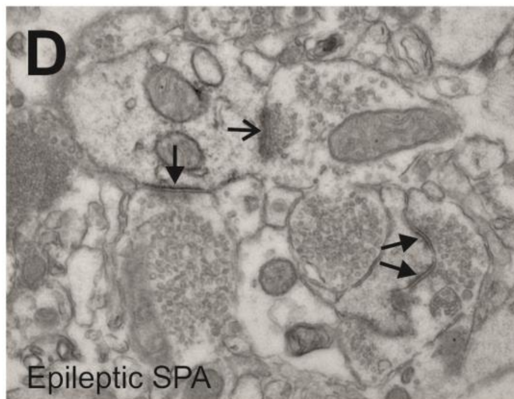
D
Epileptic SPA

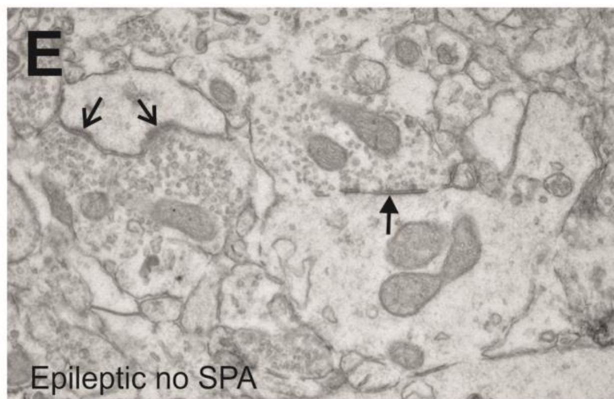
E
Epileptic no SPA

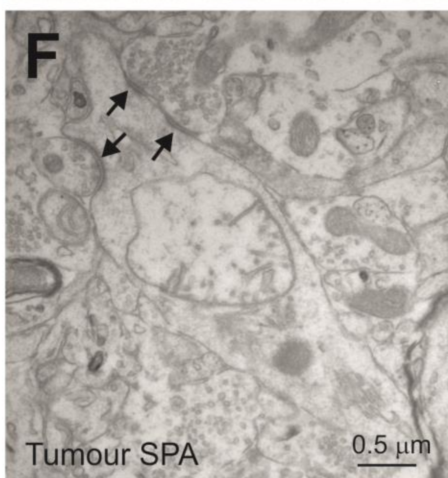
F
Tumour SPA
0.5 μm

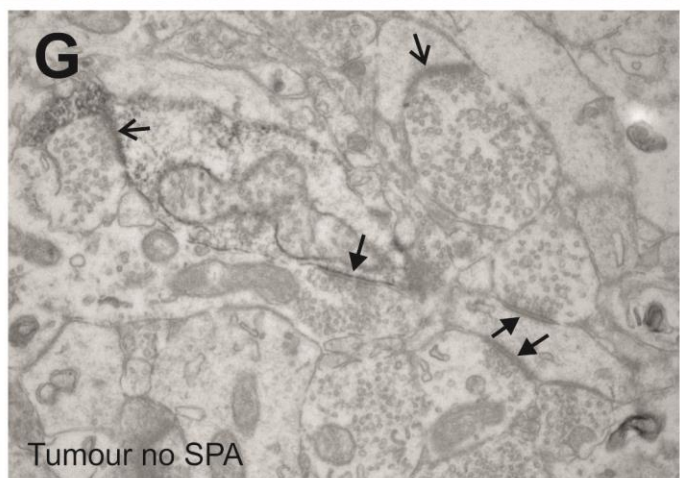
G
Tumour no SPA

Figure 5

Anatomical data related to SPA generation.

Neuron and synapse counting was performed on NeuN-stained sections (A). Neuron density (B, black boxes on A) and synapse density (C, red boxes on A) were determined in areas where SPA was recorded and in areas of the same slice where SPA could not be detected.

(B) Neuronal densities (n/mm^2) were variable in the different layers of the neocortex of epileptic and tumour patients. Neuron density was lower in epileptic than in tumour tissue, and it was slightly higher in regions with SPA than in areas lacking SPA. (C) Density of asymmetrical (excitatory) and symmetrical (inhibitory) synapses ($n/100\ \mu m^2$) in epileptic and tumour tissue. No difference was found between areas with or without SPA. The density of excitatory synapses was higher in epileptic than in tumour tissue ($p<0.001$). (D-G) Electron micrographs show asymmetrical (open arrows) and symmetrical (filled arrows) synapses from epileptic (D, E) and tumour (F, G) tissue, from areas with SPA (D, F) or without SPA (E, G).

Tables

Table 1. Patient data

Epileptic patients	**Gender**	**Age**	**Diagnosis**	**Resected cortical region**	**Duration of epilepsy**	**Stage of epilepsy**	**Distance from tumour**	**Anatomy of obtained tissue**
E1	F	22	encephalitis	parietal	1 month	A		normal/cell loss
E2	F	21	focal cortical dysplasia with glioneural heterotopia	frontal	2 years	A		dysgenetic
E3	F	18	bilateral frontal polymicrogyria	frontal	5 years	A		dysgenetic
E5	F	18	focal cortical dysplasia II B	temporal	5 years	A		dysgenetic
E6	M	51	hippocampal sclerosis	temporal	50 years	A		normal
E8	F	33	focalis corticalis dysplasia II B	occipital	31 years	A		normal+dysgenetic
E10	M	21	hippocampal sclerosis	temporal	21 years	A		normal
E11	M	29	cavernous malformation	temporal	3 years	A		N/A
E12	M	40	hippocampal sclerosis	temporal	35 years	A		normal
E13	F	53	hippocampal sclerosis	temporal	40 years	A		normal
E15	M	35	focal cortical dysplasia + hippocampal sclerosis	temporal	34 years	A		normal
E16	M	26	subependymal gliosis (dysgenesis) + hippocampal sclerosis	temporal	24 years	A		normal
E17	F	38	focal cortical dysplasia + hippocampal sclerosis	frontal	31 years	A		normal
E18	F	35	focal cortical dysplasia II B (with balloon cells)	frontal	30 years	A		normal
E21	M	56	haemangioma cavernosum	temporal	26 years	A		N/A
E23	F	33	haemangioma cavernosum	temporal	5 years	A		normal
E25	M	53	hippocampal sclerosis	temporal	24 years	A		normal
E27	M	27	hippocampal sclerosis	temporal	2 years	A		normal
E29	M	18	focal cortical dysplasia	parietal	5 years	A		dysgenetic
E30	M	30	microdysgenesis + hippocampal sclerosis	temporal	17 years	A		dysgenetic
E32	F	31	focal cortical dysplasia II B (with balloon cells)	parietal	18 years	A		dysgenetic
E34	F	18	hippocampal sclerosis	temporal	4 years	A		N/A
E35	F	37	cavernous malformation	temporal	6 years	A		N/A
E39	F	36	hippocampal sclerosis	temporal	30 years	A		N/A
E42	M	44	subpialis gliosis (dysgenesis)	frontal	22 years	A		N/A
E45	M	48	focal cortical dysplasia II B	frontal	39 years	A		N/A
Epileptic patients with	**Gender**	**Age**	**Diagnosis**	**Resected cortical region**	**Duration of epilepsy**	**Stage of epilepsy**	**Distance from tumour**	**Anatomy of obtained tissue**

tumour								
E4	M	24	ganglioglioma grade I	temporal	4 years	A	distant	normal
E14	M	53	ganglioglioma grade I	parietal	18 years	A	close	normal
E19	F	72	radionecrosis (1 year earlier: astrocytoma grade II)	frontal	2 years	C	close	normal
E20	F	33	glioblastoma grade IV	frontal	3 month	C	distant	N/A
E24	M	71	glioblastoma grade IV	frontal	1 week (1 seizure)	B	close	normal
E26	M	44	anaplastic ganglioglioma grade III	temporal	3 months (1 seizure)	C	distant	N/A
E28	F	60	anaplastic oligodendroglioma grade III, recidiva	frontal	10 years	B	close	N/A
E31	M	31	complex dysembrioplastic neuroepithelial tumour	temporal	10 years	A	distant	N/A
E33	M	63	lung adenocarcinoma metastaticum	occipital	2 weeks (1 seizure)	C	close	N/A
E40	M	32	anaplastic oligoastrocytoma grade III	frontal	4 years	A	distant	N/A
E41	F	26	radionecrosis (2 years earlier: pylocytic astrocytoma)	temporal	13 years	A	close	N/A
E44	F	32	anaplastic astrocytoma grade III	frontal	N/A (1 seizure)	C	distant	N/A
E46	F	38	ganglioglioma grade I	temporal	10 years	A	close	N/A
O42	M	72	glioblastoma multiforme	frontal	9 months (1 seizure)	A	distant	normal
T1	F	54	oligodendroglioma grade II	frontal	2 weeks (1 seizure)	B	distant	N/A
T3	F	18	anaplastic ependymoma grade III	frontal	1 month	B	distant	normal
T5	F	35	oligodendroglioma grade III	occipital	1 month (1 seizure)	B	close	infiltrated
T9	F	48	lung small cell carcinoma metastaticum	occipital	2 weeks (1 status epilepticus)	B	close	infiltrated
T10	M	44	glioblastoma multiforme, astrocytoma grade IV	temporal	3 weeks	B	distant	normal
T13	M	53	radionecrosis (6 years earlier: anaplastic oligoastrocytoma grade III)	frontal	6 years (1 seizure)	B	distant	N/A
T22	M	65	epidermoid carcinoma metastaticum	occipital	13 months (1 seizure)	C	distant	normal
T31	M	64	lung carcinoma metastaticum	temporal	3 months (1 seizure)	B	distant	normal
T46	F	68	glioblastoma grade IV	temporal	2 weeks	B	close	N/A
Tumour patients	**Gender**	**Age**	**Diagnosis**	**Resected cortical region**		**Stage of epilepsy**	**Distance from tumour**	**Anatomy of obtained tissue**
T2	M	59	glioblastoma multiforme sarcomatosum	temporal		D	close	N/A
T4	F	69	glioblastoma multiforme	temporal		D	distant	normal
T6	M	31	cavernoma, haematoma intracerebralis acuta	frontal		D	distant	normal
T7	F	58	glioblastoma multiforme, meningitis	temporal		D	close	infiltrated
T8	F	78	glioblastoma multiforme, astrocytoma grade IV	temporal		D	distant	normal
T11	F	57	glioblastoma multiforme grade IV	occipital		D	distant	normal
T12	M	59	glioblastoma, with oligodendroglioma fragments grade IV	frontal		D	close	normal
T14	M	67	lung anaplastic carcinoma metastaticum	temporal		D	close	N/A

T15	F	67	meningioma grade I	frontal		D	distant	N/A
T16	F	69	gastrointestinal adenocarcinoma metastaticum	occipital		D	close	N/A
T17	F	74	glioblastoma multiforme grade IV	parietal		D	distant	normal
T18	M	68	melanoma malignum metastaticum	parietal		D	distant	normal
T19	M	69	lung adenocarcinoma metastaticum	parietal		D	close	N/A
T20	F	59	breast carcinoma metastaticum	frontal		D	close	infiltrated
T21	F	69	kidney carcinoma metastaticum	parietal		D	distant	normal
T23	F	81	meningioma grade I	frontal		D	distant	normal
T24	M	55	lung adenocarcinoma metastaticum	temporal		D	distant	N/A
T25	F	55	glioblastoma multiforme	parietal		D	distant	N/A
T26	F	63	glioblastoma multiforme grade IV	parietal		D	close	N/A
T27	F	61	lung carcinoma metastaticum	frontal		D	distant	N/A
T28	M	49	kidney carcinoma metastaticum	occipital		D	close	N/A
T29	F	62	lung adenocarcinoma metastaticum	parietal		D	close	N/A
T32	M	79	glioblastoma multiforme grade III	temporal		D	close	N/A
T33	M	45	anaplastic astrocytoma	frontal		D	close	N/A
T34	F	64	haematoma	frontal		D	distant	N/A
T35	M	60	glioblastoma grade IV	temporal		D	distant	N/A
T38	M	82	stomach anaplastic carcinoma metastaticum	temporal		D	close	N/A
T39	M	37	centralis neurocytoma grade II	frontal		D	distant	N/A
T40	M	45	anaplastic astrocytoma grade III	temporal		D	close	N/A
T42	F	59	breast carcinoma metastaticum	frontal		D	close	N/A
T43	M	73	melanoma malignum metastaticum	temporal		D	distant	N/A
T44	F	58	breast carcinoma metastaticum	occipital		D	distant	N/A
T45	F	56	glioblastoma grade IV	occipital		D	distant	N/A

F=female, M=male, N/A=not available, Stage of epilepsy: A: pharmacoresistant epilepsy, B: treatable epilepsy, C: no need for medication, D: no epilepsy

Table 2. SPA occurrence in neocortical slices deriving from different lobes of the brain

	All epileptic patients			Epileptic patients without tumour			Epileptic patients with tumour			Tumour patients without epilepsy		
	n	Ratio of slices generating SPA (%, sum of slices with SPA/sum of all slices)	Ratio of slices generating SPA (%, by patient, mean±SD)	n	Ratio of slices generating SPA (%, sum of slices with SPA/sum of all slices)	Ratio of slices generating SPA (%, by patient, mean±SD)	n	Ratio of slices generating SPA (%, sum of slices with SPA/sum of all slices)	Ratio of slices generating SPA (%, by patient, mean±SD)	n	Ratio of slices generating SPA (%, sum of slices with SPA/sum of all slices)	Ratio of slices generating SPA (%, by patient, mean±SD)
Frontal lobe	15	35.2	35.0±29.4	6	37.1	42.7±34.4	9	34.0	29.8±26.5	10	34.0	34.2±29.2
Occipital lobe	4	41.2	35.0±27.4	1	66.7	66.7±0.0	3	27.3	24.4±21.4	5	36.4	31.7±31.1
Parietal lobe	5	47.2	48.7±25.4	3	63.6	66.1±12.1	2	21.4	22.5±3.5	7	33.3	30.3±19.3
Temporal lobe	25	54.3	55.5±27.7	16	59.3	58.5±24.5	9	46.3	50.0±33.7	11	25.4	24.3±27.8
Total	**49**	**46.6**	**46.8±28.9**	**26**	**55.0**	**56.1±25.9**	**23**	**37.1**	**36.4±29.0**	**33**	**31.1**	**29.7±26.3**

Table 3. Relationship of SPA occurrence and aetiology

		Number of patients	Ratio of slices generating SPA (%, sum of slices with SPA/sum of all slices)	Ratio of slices generating SPA (% by patient, mean±SD)
Epileptic	Dysgenesis	13	54.9	58.3±28.6
	Hippocampal sclerosis	8	57.1	56.1±17.5
	Other	5	52.0	50.3±34.0
	Tumour	23	37.1	36.4±29.0
	Total	**49**	**46.6**	**46.8±28.9**
Tumour	Glial tumour	31	38.1	38.7±28.6
	Carcinoma metastasis	18	23.7	20.6±21.3
	Other tumour	7	35.9	35.0±29.0
	Total	**56**	**33.5**	**32.4±27.4**

Table 4. SPA distribution across neocortical layers. Number of SPAs (and IIDs) are provided appearing as single or as part of multiple SPAs, in the different layers of the human neocortex.

SPAs in neocortical layers	Epileptic patients without tumour				Epileptic patients with tumour				Tumour patients without epilepsy		
	Single SPA	Multiple SPA	Total SPA (%)	IID	Single SPA	Multiple SPA	Total SPA (%)	IID	Single SPA	Multiple SPA	Total SPA (%)
Supra	35	41	76 (56.3%)	0	18	17	35 (49.3%)	0	33	17	50 (53.8%)
Supra-gran	12	12	24 (17.8%)	0	6	6	12 (16.9%)	1	6	7	13 (14.0%)
Gran	5	10	15 (11.1%)	1	3	4	7 (9.9%)	0	3	11	14 (15.1%)
Gran-infra	0	6	6 (4.4%)	5	0	1	1 (1.4%)	0	1	3	4 (4.3%)
Infra	2	7	9 (6.7%)	2	1	7	8 (11.3%)	0	2	8	10 (10.8%)
Entire	2	3	5 (3.7%)	0	4	4	8 (11.3%)	0	0	2	2 (2.2%)
Total number of SPAs or IIDs	**56**	**79**	**135**	**8**	**32**	**39**	**71**	**1**	**45**	**48**	**93**
Number of slices with SPAs or IIDs (% of slices with SPA/IID)	**56 (66.7%)**	**28 (33.3%)**	**84 (54.9%)**	**6 (7.1%)**	**32 (65.3%)**	**16 (32.7%)**	**49 (36.6%)**	**1 (2.0%)**	**45 (75%)**	**15 (25%)**	**60 (30.9%)**
Total number of examined slices	**153**				**134**				**194**		

Supra = supragranular (layers I-III) layers, Supra-gran = supragranular+granular (layer IV) layers, Gran = granular layer, Gran-infra = granular+infragranular (layers V-VI) layers, Infra = infragranular layers, Entire = entire width of the neocortex, involving supragranular+granular+infragranular layers, see also Fig. 2)

Table 5. Network properties of human neocortical SPAs and IIDs.

		Number of SPAs/IIDs analysed	Recurrence frequency (Hz)	Largest LFPg amplitude (μV)	Width at half of the maximal amplitude (ms)	Asymmetry at half of the maximal amplitude (right/left)	Largest CSD amplitude (μV)	Largest MUA amplitude (μV)
Epileptic SPA	**Total SPA**	**46**	**1.03 [0.91 1.22]** **(1.20 ± 0.71)**	**23.22 [18.59 27.01]** **(27.31 ± 17.23)**	**26.35 [23.75 31.85]** **(34.09 ± 20.43)**	**1.55 [1.45 1.77]** **(1.72 ± 0.64)**	**14.30 [12.92 16.97]** **(16.76 ± 8.79)**	**1.06 [0.77 1.12]** **(1.49 ± 1.46)**
	Supragran SPA	38	1.04 [0.88 1.31] (1.22 ± 0.67)	23.38 [18.82 28.72] (28.25 ± 18.14)	26.35 [23.60 31.65] (33.89 ± 21.53)	1.63 [1.46 1.91] (1.79 ± 0.62)	14.30 [12.91 17.77] (17.14 ± 9.03)	1.10 [0.93 1.42] (1.65 ± 1.55)
	Infragran SPA	7	0.99 [0.13 1.74] (1.06 ± 0.96)	17.67 [14.77 27.81] (22.65 ± 12.87)	24.70 [22.75 39.30] (31.53 ± 12.40)	1.09 [0.92 1.57] (1.23 ± 0.54)	13.56 [8.66 18.35] (14.86 ± 8.50)	0.75 [0.28 1.06] (0.68 ± 0.38)
Tumour SPA	**Total SPA**	**48**	**1.06 [0.90 1.38]** **(1.18 ± 0.60)**	**15.41 [12.82 20.47]** **(18.40 ± 10.48)**	**23.05 [21.00 25.85]** **(24.98 ± 11.23)**	**1.46 [1.20 1.59]** **(1.62 ± 0.78)**	**10.08 [8.14 12.98]** **(12.05 ± 6.34)**	**0.90 [0.68 1.17]** **(1.29 ± 1.17)**
	Supragran SPA	36	1.08 [0.89 1.39] (1.16 ± 0.58)	16.09 [12.74 20.61] (18.64 ± 10.51)	23.70 [21.10 27.40] (26.10 ± 11.98)	1.41 [1.15 1.57] (1.58 ± 0.80)	11.06 [8.50 13.19] (12.36 ± 6.46)	0.73 [0.57 1.09] (1.11 ± 1.12)
	Infragran SPA	11	0.98 [0.57 1.81] (1.17 ± 0.69)	13.08 [7.39 25.67] (16.97 ± 11.07)	21.00 [17.70 27.55] (21.58 ± 8.50)	1.65 [1.03 2.21] (1.75 ± 0.78)	7.84 [6.45 15.43] (10.70 ± 6.24)	1.76 [0.87 2.93] (1.90 ± 1.22)
Epileptic IID		**8**	**0.05 [0.02 0.14]** **(0.10 ± 0.13)**	**74.36 [60.16 100.34]** **(74.70 ± 21.99)**	**37.00 [19.30 52.55]** **(40.69 ± 20.19)**	**1.77 [1.30 2.62]** **(1.92 ± 1.04)**	**42.97 [40.86 52.21]** **(46.09 ± 10.05)**	**5.81 [1.66 8.94]** **(6.46 ± 4.57)**
Significant differences			Epi SPA > Epi IID p<0.0001	Epi SPA > Tumour SPA p<0.01 Epi supra > Tumour supra p<0.01 Epi IID > Epi SPA p<0.0001	Epi SPA > Tumour SPA p<0.05	n.s.	Epi SPA > Tumour SPA p<0.01 Epi supra > Tumour supra p<0.05 Epi IID > Epi SPA p<0.0001	Epi IID > Epi SPA p<0.01

We provided median [95% confidence interval of the median] (mean±SD), since none of the examined parameters showed Gaussian distribution.
Epi=epileptic, n.s.=non-significant, Supragran = supra, supra-gran and gran SPAs, Infragran = gran-infra and infra SPAs

Table 6. High frequency oscillations (HFO) during SPA and IID. Ripple (130-250 Hz) and fast ripple (300-800 Hz) frequencies were examined in neocortical slices with SPA and IID.

			Number of SPAs/IIDs (n)							
		Total (n)	**With HFO**	**Without HFO**	**With ripple activity**	**With fast ripple activity**	**Ripple frequency (Hz)**	**Ripple power**	**Fast ripple frequency (Hz)**	**Fast ripple power**
Epileptic SPA	**Total**	**46**	**38 (82.6%)**	**8 (17.4%)**	**35 (76.1%)**	**29 (63.0%)**	**178.00 [161.00 193.00] (180.89 ± 37.39)**	**1.77 [1.45 2.31] (2.07 ± 1.03)**	**440.00 [400.00 512.00] (475.55 ± 130.24)**	**1.44 [1.15 1.69] (1.75 ± 0.91)**
	Supragran SPA	38	32 (84.2%)	6 (15.8%)	29 (76.3%)	24 (63.2%)	180.00 [164.00 193.00] (184.14 ± 36.99)	1.70 [1.45 2.24] (2.09 ± 1.06)	437.50 [400.00 534.00] (486.75 ± 136.83)	1.43 [1.15 1.73] (1.67 ± 0.91)
	Infragran SPA	7	6 (85.7%)	1 (14.3%)	6 (85.7%)	5 (71.4%)	161.50 [127.50 206.50] (165.17 ± 38.57)	2.19 [0.82 2.84] (1.95 ± 0.95)	471.00 [329.00 500.00] (421.80 ± 81.94)	2.26 [0.91 3.07] (2.15 ± 0.87)
Tumour SPA	**Total**	**48**	**33 (68.8%)**	**15 (31.3%)**	**30 (62.5%)**	**26 (54.2%)**	**198.00 [187.00 214.50] (208.83 ± 43.35)**	**2.02 [1.61 2.87] (2.34 ± 1.08)**	**462.50 [438.00 573.00] (508.81 ± 110.31)**	**1.47 [1.31 2.20] (1.83 ± 0.80)**
	Supragran SPA	36	24 (66.7%)	12 (33.3%)	21 (58.3%)	19 (52.8%)	194.00 [179.00 219.00] (209.86 ± 48.24)	1.80 [1.42 2.71] (2.17 ± 1.16)	522.00 [445.00 624.00] (535.69 ± 113.84)	1.36 [1.20 1.69] (1.60 ± 0.70)
	Infragran SPA	11	8 (72.7%)	3 (27.3%)	8 (72.7%)	6 (54.5%)	208.50 [197.00 248.00] (208.75 ± 32.71)	3.15 [2.56 3.37] (2.89 ± 0.68)	433.50 [381.00 488.00] (434.17 ± 62.96)	2.77 [2.00 3.10] (2.62 ± 0.67)
Epileptic IID		**8**	**7 (87.5%)**	**1 (12.5%)**	**6 (75.0%)**	**7 (87.5%)**	**147.95 [135.25 226.30] (169.83 ± 52.33)**	**4.90 [3.69 6.04] (4.88 ± 1.09)**	**397.50 [317.40 689.00] (459.46 ± 168.76)**	**4.01 [3.37 4.23] (4.11 ± 1.25)**
Significant differences			n.s.		n.s.	n.s.	Epi SPA < Tumour SPA p<0.01	Epi SPA < Epi IID p<0.001	n.s.	Epi SPA < Epi IID p<0.001

Epi=epileptic, n.s.=non-significant, Supragran = supra, supra-gran and gran SPAs, Infragran = gran-infra and infra SPAs

Table 7. Characteristics of intracellularly recorded cells

Cells from epileptic tissue	Cortex	Cell location (anatomically identified, layer)	RMP (mV)	Spontaneous firing	SPA location (layer)	Response to SPA	Firing during SPA (% of events)
E3Cell1	frontal	supra	-58.7	silent	no SPA	-	
E3Cell2	frontal	infra (reconstructed, L5)	-55.5	firing	no SPA	-	
E5Cell1	frontal	infra	-54.0	silent	no SPA	-	
E5Cell2	frontal	infra	-54.9	silent	no SPA	-	
E8Cell1	occipital	supra	-54.9	firing	supra-gran	depolarizing+firing	43.5%
E10Cell1	temporal	infra (reconstructed, L5)	-52.9	firing	supra	no response	
E13Cell2	temporal	infra (identified, L5)	-58.0	silent	infra	depolarizing+firing	14.3%
E13Cell3	temporal	supra (identified, L3)	-68.0	silent	supra	depolarizing	
E15Cell1	temporal	supra	-59.5	firing	supra-gran	depolarizing+firing	96.5%
E15Cell2	temporal	supra	-59.8	firing	supra	depolarizing+firing	55.6%
E15Cell3	temporal	supra (identified, L2)	-67.4	silent	supra-gran	depolarizing	
E16Cell1	temporal	supra	-55.5	silent	supra	depolarizing	
					gran	no response	
					gran-infra	depolarizing	
E16Cell2	temporal	supra	-52.4	silent	supra	depolarizing	
					gran	depolarizing	
					gran-infra	depolarizing	
E16Cell3	temporal	supra	-55.0	firing	supra	depolarizing+firing	29.8%
					gran	no response	
					gran-infra	depolarizing	
E16Cell4	temporal	infra (reconstructed, L5)	-75.0	silent	supra	no response	
					gran	no response	
					gran-infra	depolarizing+firing	36.3%
E17Cell1	temporal	supra	-53.1	firing	supra	hyperpolarizing	
E17Cell2	temporal	supra	-52.2	firing	supra	depolarizing+firing	86.7%
Total (n=17)			**-58.3±6.5**	**9 silent/8 firing**		**11 depolarizing** **1 hyperpolarizing**	**51.8±30.1%** **(7/12 cells firing)**
Cells from tumour tissue	**Cortex**	**Cell location (anatomically identified, layer)**	**RMP (mV)**	**Spontaneous firing**	**SPA location (layer)**	**Response to SPA**	**Firing during SPA (% of events)**
T2Cell1	frontal	supra	-53.1	firing	supra	hyperpolarizing	

T2Cell2	frontal	supra	-54.6	firing	supra	biphasic+firing	7.0%
T2Cell3	frontal	supra (reconstructed, L2)	-71.0	firing	gran	depolarizing+firing	11.1%
T8Cell1	temporal	supra (identified, L3)	-64.2	silent	supra	hyperpolarizing	
T8Cell2	temporal	supra	-64.1	firing	supra	biphasic+firing	24.0%
T11Cell1	occipital	supra	-50.1	firing	supra	depolarizing+firing	21.7%
T14Cell1	frontal	supra	-54.7	firing	supra	hyperpolarizing	
T14Cell2	frontal	infra	-55.3	firing	supra-gran	biphasic+firing	17.6%
T15Cell2	frontal	infra	-51.1	firing	no SPA	-	
T17Cell1	parietal	supra	-52.0	silent	no SPA	-	
T17Cell2	parietal	supra	-75.0	silent	supra	depolarizing	
T18Cell1	parietal	supra	-68.0	firing	supra	no response	
					gran	no response	
					supra2	depolarizing+firing	10.0%
T23Cell1	parietal	supra	-56.7	silent	supra	depolarizing	
T23Cell2	parietal	supra	-61.9	firing	supra	depolarizing+firing	39.3%
T26Cell1	parietal	supra	-54.8	firing	supra	hyperpolarizing	
T38Cell1	parietal	supra (identified, L3)	-50.2	firing	no SPA	-	
Total (n=16)			**-58.5±7.8**	**5 silent/11 firing**		**6 depolarizing 3 biphasic 4 hyperpolarizing**	**18.7±11.0% 7/13 cells firing**

Supra: supragranular, infra: infragranular, L2, L3, L5: layer 2, 3, 5

Table 8. Neuron density in the neocortex generating or not generating SPA

	Epileptic			Tumour		
	Number of cells counted	Neuron density (n/mm^2) SPA	Neuron density (n/mm^2) No SPA	Number of cells counted	Neuron density (n/mm^2) SPA	Neuron density (n/mm^2) No SPA
Layer I	367	476±81	389±46	116	705±199	398±10
Layer II	3 055	3 506±707	3 129±98	939	4 327±57	3 170±965
Layer III	3 415	1 866±81	1 683±8	2 727	2 132±27	1 821±717
Layer IV	2 890	3 251±77	3 162±227	1 840	3 938±179	3 700±1 172
Layer V	3 913	1 462±107	1 428±112	2 292	1 753±391	1 496±778
Layer VI	562	361±223	372±97	719	360±356	421±334
Total	**14 202**	**1 820±1 338**	**1 694±1 244**	**8 633**	**2 202±1 635**	**1 834±1 374**

Table 9. Number of excitatory (asymmetrical) and inhibitory (symmetrical) synapses in areas generating or not generating SPA.

	Examined area (µm^2)	Excitatory synapses		Inhibitory synapses		All synapses		Ratio of excitatory / inhibitory synapses
		Number (% of total)	Number per 100 µm^2	Number (% of total)	Number per 100 µm^2	Number	Number per 100 µm^2	
Epileptic SPA	2 904	199 (49.4±5.3%)	7.3±2.2	204 (50.6±5.3%)	7.3±1.9	403	14.6±3.9	0.99±0.21
Epileptic No SPA	2 232	165 (46.2±9.2%)	7.4±2.6	189 (53.8±9.2%)	8.4±2.2	354	15.8±4.1	0.89±0.31
Tumour SPA	3 393	149 (37.8±7.7%)	4.3±1.5	233 (62.2±7.7%)	6.8±0.7	382	11.1±2.0	0.62±0.19
Tumour No SPA	2 751	112 (38.0±5.2%)	4.0±0.7	185 (62.0±5.2%)	6.6±1.6	297	10.7±2.0	0.62±0.14